Integrated optimization of charging infrastructure, electric bus scheduling and energy systems

Transportation Research Part D 141 (2025) 104664

Contents lists available at ScienceDirect

Transportation Research Part D

journal homepage: www.elsevier.com/locate/trd

Integrated optimization of charging infrastructure, electric bus scheduling and energy systems

Arsalan Najafi [a,b], Kun Gao [a,*], Omkar Parishwad [a], Georgios Tsaousoglou [c], Sheng Jin [d], Wen Yi [e]

[a] Department of Architecture and Civil Engineering, Chalmers University of Technology, Gothenburg SE-412 96, Sweden
[b] Department of Electrical Engineering Fundamentals, Wroclaw University of Science and Technology, 50-370 Wrocław, Poland
[c] Department of Applied Mathematics and Computer Science, Technical University of Denmark, Denmark
[d] Institute of Intelligent Transportation Systems, College of Civil Engineering and Architecture, Zhejiang University, Hangzhou 310058, China
[e] Faculty of Construction and Environment, The Hong Kong Polytechnic University, Hung Hom, Hong Kong, China

ARTICLE INFO

Keywords:
Electric transport
Charging infrastructure
Charging scheduling
Renewable energy
Benders decomposition

ABSTRACT

The adoption of Battery Electric Buses (BEBs) in electric public transit systems presents a significant opportunity for advancing sustainable transportation. This study introduces a holistic framework for joint optimization of charging infrastructure, charging scheduling, and integration of renewable energy resources (RES), considering impacts on Power distribution network (PDN). To address the complex optimization, a decomposition approach is employed to linearize the problem and divide it into master and subproblems for efficient resolution. A case study in Skövde, Sweden demonstrates that the proposed methodology optimizes charging infrastructure deployment and scheduling to reduce the overall system costs. Meanwhile, high charging demand from BEBs in some periods to fulfil operation scheduling may result in violation of technical constraints of the PDN (more than 4%), without RES. The incorporation and optimization of RES with battery energy storage can cater to spatiotemporal charging demand of BEB while enhancing stability and safety of PDN.

1. Introduction

The urgent need to reduce greenhouse gas emissions from the transport sector, which account for over 24% of global CO_2 emissions, has accelerated the global shift towards sustainable transportation. In response to this environmental challenge, Battery Electric Buses (BEBs) have emerged as one of the significant contributors to this transition, offering a viable and eco-friendly alternative to traditional fossil fuel-based public transit. The proliferation of BEBs in public transit systems globally signifies a notable shift towards greener and more sustainable urban mobility (Cui et al., 2023; Zeng and Qu, 2023). BEBs are increasingly favoured for their economic imperative to lower operating costs over fuel efficiency and maintenance needs (Pragaspathy et al., 2022; Zhang et al., 2022). Despite these benefits, integrating BEBs into existing urban infrastructures poses significant challenges that impede their broader adoption and efficient operation (Perumal et al., 2022; Dong et al., 2024). One major obstacle is the high upfront cost of BEBs. Despite the long-term savings on fuel and maintenance, the initial investment for BEBs is substantially higher than traditional buses, especially for public transit authorities operating under tight budget constraints.

Additionally, the operational complexity of BEBs, particularly in charging scheduling, adds another layer to the challenge. Efficiently managing BEB charging scheduling is crucial to ensure that buses are adequately charged and available for service without

* Correspondence to: Sven Hultins Gata, 41296, Gothenburg, Sweden.
E-mail address: gkun@chalmers.se (K. Gao).

https://doi.org/10.1016/j.trd.2025.104664
Received 1 August 2024; Received in revised form 13 February 2025; Accepted 13 February 2025
Available online 28 February 2025

Nomenclature

A. Sets and indices

$t, \mathcal{T}$	Index and set of times within the whole horizon
$i, j, \mathcal{S}$	Indices and set of service trips
$o, \mathcal{O}$	Index and set of first trip leaving origin nodes
$d, \mathcal{D}$	Index and set of last trip arriving at destination nodes
$\mathcal{OS}$	Set of the union of origin node and services trips
$\mathcal{SD}$	Set of the union of services trips and destination node
$\mathcal{S}^{Dyn}$	Dynamic set of the service trips going to the depot
$k, \mathcal{K}$	Index and set of charger types
$b, \mathcal{B}$	Index and set of nodes of power distribution network
$n, \mathcal{N}$	Index and set of nodes of the bus transit system
$\mathcal{B}_r$	Set of candidate nodes of the power distribution network, coupled to the transit system, to install renewable energy resources (RES) and battery electric storage (BES)
$w, \mathcal{W}$	Index and set of scenarios.
$\mathcal{N}_b$	Set of transit system nodes connected to PDN node b excluding depot ($\mathcal{N}_b \subset \mathcal{N}$)
$\mathcal{N}_b^d$	Set of depots connected to PDN node b ($\mathcal{N}_b^d \subset \mathcal{N}$)

B. Parameters

p^{CMax}	Maximum charging capacity of a BEB
$\underline{u}_i, \overline{u}_i$	Start/end time of trip i
$u^{\mathrm{L}}, u^{\mathrm{F}}$	Last and first trip time in the timetable
τ_{ij}^{S2D}	Deadhead trip time from trip i to depots ($j \in \mathcal{D}$)
τ_i^{O2S}	Deadhead trip time from the origin to trip i
τ_i^{DH}	Deadhead trip time between after finishing trip i
τ_i	Travel time of trip i
$\underline{\lambda}, \overline{\lambda}$	Minimum and maximum charging percentage
Q	Energy capacity of a BEB.
c_{oi}^{O2S}	Energy consumption of deadhead trip from the depot to start the service trips
c_i^{SL}	Energy consumption during trip i
c_{ij}^{S2D}	Energy consumption of deadhead trip from trip i to the depots ($j \in \mathcal{D}$)
$D_{b,t}^{\mathrm{P}}, D_{b,t}^{\mathrm{Q}}$	Active and reactive loads of b at t
r_b	Resistance of branch $b, b+1$.
$\overline{\mathrm{V}}, \underline{\mathrm{V}}$	Upper and lower bound of voltage.
x_b	Reactance of branch $b, b+1$
$P_{wt}^{PV,Max}$	Maximum generation of RES in terms of weather prediction
PV^{CapMax}	Maximum generation of RES in terms of land use
ρ	Cost of procuring a BEB
ρ_{fA}	Fixed cost of the area of planning charging station
ρ_v	Variable cost of the area of planning charging station
C^{CW}	Capital cost of installing RES
M	Sufficiently big number
ρ_t^{M}	Electricity market price
$\eta_b^{\mathrm{c}}, \eta_b^{\mathrm{d}}$	Charging/discharging efficiency of the BES
$\overline{\Theta}, \underline{\Theta}$	Upper/lower allowable percentage of the energy in the BES
$\overline{\Psi}$	Upper-level allowable percentage for charging and discharging in the BES
ir	Interest rate
A^{Ter}	Area of the required to install chargers at depot or bus stations
P^{VF}	Present value factor

N^{Day}, ny	Number of days included in the simulation and number of years of horizon planning
ξ_w	Probability of scenario w
PF	Voltage deviation penalty factor

C. Variables

x_{ij}	A binary variable to assign a trip to a bus
$\mathrm{I}^{Ch}_{j,i,k}$	A binary variable to assign a charger of after finishing trip j to the bus (trip) i by charger k
$\mathrm{N}^{Ch}_{n,k}$	An integer variable showing the number of chargers type k at bus station n
p^{Ter}_{injt}	Received power by the en-route charging station by bus at t
p^{Dep}_{ijt}	Received power by the depots by bus at t
δ_{in}	Binary variable to deploy a charger
I_n	Binary variable to locate a charger
p^{TMax}_n	Capacity installed on stations connected to node n
p^{DMax}_n	Capacity installed on depot connected to node depot d
e^{Ter}_{inj}	Received energy by the en-route charging station by the bus
e^{Dep}_{ij}	Received energy at the depots by the bus
$e^{\max}$	Total energy received by all BEBs in the depot
$\mathrm{P}^{Ch,\max}_k$	Maximum power capacity of the charger type k
q_{oi}	Energy of the bus when it departs the depot
q_{ij}	Energy of the bus when after trip i and exactly before starting trip j
$\tilde{q}_i$	Amount of remaining energy in the battery after finishing trip i
$Q^{\mathrm{CAP}}_{b,t}$	Reactive power of capacitor banks at PDN node b at t and s
$V_{b,w,t}$	Voltage magnitude of PDN node b, scenario w and timeslot t
p^{DN2B}_{wtb}	Purchased electricity by the bus transit system from the PDN to supply the charging demand at PDN node b, scenario w and timeslot t
$V^{\mathrm{DEV}}_{b,w,t}$	Voltage deviation from the minimum bound of PDN node b at t and W
$P^{\mathrm{RES}}_{b,w,t}$	RES generation at PDN node b, timeslot t and scenario w
$P^{\mathrm{RES,BES}}_{b,w,t}$	RES generation storing in the BES at PDN node b, timeslot t and scenario w
$P^{\mathrm{RES,D}}_{b,w,t}$	RES generation directly supporting the demands at PDN node b, timeslot t and scenario w
PV^{Cap}_b	RES capacity installing on PDN node b
p^{Ch}_{wtb}, p^{Dch}_{wtb}	Charging/discharging of the BES at node b, timeslot t and scenario w
e^{BES}_{wtb}	State of charge of the BES at node b, timeslot t and scenario w
$\overline{\mathrm{E}}_b$	Installing capacity of the BES at PDN node b
$P^{\mathrm{BEB}}_{b,w,t}$	Charging demand
I^{RES}_b	Binary variable to assign RES to PDN node b
I^{Ch}_{wtb}	Binary variable to assign either charging or discharging to the BES at PDN node b
IC, OC	Total investment/operation cost
UB/LB	Upper/lower bound in benders decomposition
α	Objective function of the master problem
$\varrho_i, \varpi_{kj}, \vartheta_{ij}$	Dual variables of bus scheduling.
$\varsigma_{kij}, \varphi_{kijv}$,	Dual variables of charger deployment

disrupting transit operations (e.g. fulfilling the planned timetables of bus routes). This requires meticulous planning and scheduling optimization of charging times and locations, considering factors such as route length, battery capacity, and spatiotemporal availability of charging infrastructure. This complexity is heightened by the need to balance operational efficiency with the limitations of current battery technology. Failing to address these challenges efficiently puts the system at risk of operational delays and also reduces the overall reliability and efficiency of the BEB fleet (Liu et al., 2021), potentially undermining the benefits of transitioning to electric buses. Furthermore, the increasing energy demand due to the widespread adoption of BEBs may significantly impact the Power Distribution Network (PDN), considering its capacity and resilience. The demand for electricity, especially during peak periods, can strain the grid, leading to voltage drops and potential instability (Mohamed et al., 2017). This issue is compounded by the variable nature of renewable energy sources, which are often proposed as a clean energy solution for powering BEBs. Many studies (Hache and Palle, 2019; Mirzaei et al., 2019; Raza et al., 2023) highlight complexities and challenges, including technical aspects and market and financing issues, associated with integrating renewable energy sources into power networks.

While existing studies have made commendable strides in planning to charge infrastructure and BEB scheduling and in coupling BEB transit systems and PDNs, a significant gap remains in modelling the effect of charging demands on the PDN's safe and efficient operations and considering this effect in infrastructure planning and optimization. The effective modelling and consideration of the charging demands from BEB transit system are critical, as they pose an additional load of significant magnitude for the power distribution network, which may result in a drop in the voltage of PDN nodes. In many European cities, the demand from BEBs was not accounted for in the initial planning of PDNs. Such issues call for accurate coupled modelling and optimization of the charging schedule and infrastructure of BEBs, constrained by PDN capacities to ensure that there will be no congestion or voltage problems in the PDN. Towards counter-balancing the additional loads introduced by the BEB transit system, we examine the deployment of RES (herein photovoltaics-PVs) alongside energy storage systems as an integral part of the BEB transit system development, which aims to mitigate the adverse impacts of high charging demand from BEBs on PDNs in electricity usage peak hours. The proposed model better comprehends the couplings between the BEB transit system, the PDN and renewable energy sources (RES). In addition, the proposed framework is a non-linear and complex problem. Therefore, it is necessary to make the problem solvable by the off-the-shelve solvers. We have presented a decomposition method to not only linearize the problem but also to reduce the computational burden of the problem. To sum up, we summarize the contributions of the paper as follows.

- We introduce a novel approach for joint planning of BEB charging infrastructure and scheduling coupled with the PDN, extending the current practices (e.g., He et al. (2023)) which solely concentrates on BEB transit system. This comprehensive model comprehensively encompasses all three aspects: infrastructure planning, BEB scheduling, and PDN integration.
- We address the planning of PV panels and BESs as a sustainable solution to complement the BEB system deployment such that the coupled BEB-PDN system is planned in a safe, efficient, and sustainable manner by mitigating excessive charging demand of BEBs on the PDN.
- We propose a decomposition method to linearize and reduce the computational burden of the problem.

The following parts are organized as follows. First, we provide the system model in Section 3, describing the problem, mathematical modelling of the BEB scheduling and constraints, the PDN model, RES and BES planning model, as well as the objective function. The solution methodology is given in Section 4, including linearization and a decomposition methodology towards remedying computational challenges. In Section 5, the results and discussion are given, followed by the conclusion in Section 6.

2. Literature review

In urban transit systems, research on BEB systems has evolved across three key areas: charging infrastructure planning combined with BEB scheduling-charging optimization, and integrated modelling of PDN for BEB transit systems.

The *first category*, charging infrastructure planning, delves into the location, capacity, and charging infrastructure. Many studies have laid a solid foundation for optimizing charging schedules and infrastructure planning under demand uncertainty. Studies (Wu et al., 2021; Chen et al., 2018) reveal the complexities and cost considerations in developing effective charging networks, emphasizing the need for strategic power load management. Other studies (He et al., 2022b; Al-Saadi et al., 2022) demonstrate the economic benefits of intelligent charging scheduling strategies, particularly in relation to time-of-use electricity prices. An (2020) implemented a stochastic integer program to optimize charging station locations and bus fleet size, addressing demand uncertainty. These studies also suggest that integrating fast-charging infrastructure has minimal impact on power quality. A study (He et al., 2020) showcased a network modelling framework of effectively minimizing charging costs and enhances operational flexibility. However, these approaches lack adaptability to real-time urban transit demands, such as varying passenger loads and traffic conditions. Additionally, while studies (Basma et al., 2021; Al-Saadi et al., 2022) have explored the power demand and grid compatibility, there is a lack of focus on integrating environmental sustainability considerations into the planning process. This gap extends to the broader integration of charging infrastructure planning within the overall urban transit system design, as noted in other research (Liu et al., 2019; El-Taweel et al., 2022). These findings underscore the need for comprehensive and dynamically adaptive models in BEB charging infrastructure planning. Such models should consider power demand, cost efficiency, and grid compatibility, contributing to developing resilient and sustainable urban transit systems.

The *second category*, integrated planning and scheduling optimization, explores the operational aspects of BEBs, combining infrastructure planning with scheduling strategies. The integrated planning and scheduling problem mostly combines the planning of charging location and size with the charging scheduling of BEBs. Relevant studies highlight the need for dynamic scheduling responsive to urban transit demands (Duan et al., 2023; He et al., 2023). Key findings emphasize accurate energy consumption assessment and real-time smart charging for efficient fleet scheduling (Verbrugge et al., 2021; Zhao et al., 2018). Other research points to the economic advantages of optimized charging scheduling, considering factors like time-of-use pricing, passenger flow, and road conditions (He et al., 2022b; Guo et al., 2021). Li et al. (2024) proposed a joint wireless charging infrastructure planning and charging scheduling approach to optimize the deployment of dynamic charging stations under a time-of-use tariff mechanism. Similarly, Nath et al. (2024) examined joint charging infrastructure planning and charging scheduling, incorporating decisions on assigning buses to trips and determining when and where to charge them. However, their study overlooked the impact of these decisions on the power grid. An integrated charging infrastructure planning and charging scheduling was proposed in He et al. (2022a). It considered two stages to solve the problem. The integrated model was solved in the first stage to obtain the optimal charging infrastructure and schedule values. Then, the real-time uncertainty of the arrival time of buses was solved through a rolling horizon approach. The joint planning and scheduling were addressed in Gairola and Nezamuddin (2023) to find the charging station configuration battery size while the schedules were predetermined. A joint optimization approach was suggested in Hu et al. (2022)

to locate charges on stations and schedule the charging of BEBs by focusing on uncertainties stemming from passengers alighting and boarding as well as travel time. Although it also considered fast charging as an en-route solution, disregarding the charging demand effect on PDN, which may create another peak in the PDN. Similarly, Wang et al. (2023) proposed an integrated solution for fast charging planning infrastructure and battery scheduling, disregarding the PDN. The main focus of the study was to give an approach to consider the conflict of charging during dwelling on stations as well as considering the degradation cost due to the use of fast chargers. Zhou et al. (2022) suggested an approach to integrate the planning of chargers and scheduling of the batteries. The battery energy consumption was modelled precisely by incorporating various factors in energy consumption, e.g., the weight of the batteries. However, the interaction with the PDN was only addressed through the time-of-use prices. Some studies have specifically focused on scheduling BEBs, delving into greater detail about scheduling aspects. For instance, the heterogeneity of BEBs in scheduling was explored in Zhou et al. (2024). Additionally, Avishan et al. (2023) examined the BEB scheduling and procurement problem, considering the uncertainties in energy consumption and travel time.

The *third category* focuses on coupling the BEB transit system with PDNs. This stream of research deals with the challenges of increased electricity demand and renewable energy integration (Moghaddam et al., 2019). Notable work in this category includes the development of improved equilibrium optimization algorithms and strategies for enhancing PDN performance (El-Ela et al., 2021). Studies also highlight the benefits of integrating photovoltaics (PVs) with battery electric storage (BESs) in PDNs, reducing costs and CO_2 emissions (Shaheen et al., 2021). The interactions of BEB transit systems and PDNs were investigated in several studies to fulfil various purposes. In Lin et al. (2019), an approach for large-scale fast charging station-planning problems was proposed for coupling with power systems disregarding the BEB scheduling. The solution provides a multi-stage planning of charging infrastructure to popularize BEB gradually. The power system was regarded as the upstream of the BEB transit system, while the real influence of the charging demands on the power system was not addressed due to the neglect of the charging schedule. The restoration problem of PDNs with the integration of the BEB transit system was addressed in Wu et al. (2023). Although the electrical part was developed in detail, the transportation part was limited to the scheduling of the BEB transit system to meet the goals of the PDN operator. In a similar work, Li et al. (2021) proposed a framework to schedule and use the idle buses as feed power back to the PDN to restore the PDN in case of need. The profitability of bus-to-grid was investigated in Fei et al. (2023) to explore whether the BEB transit system can participate in the electricity market and earn profit in two ways. First, to earn revenues by discharging the BEB and selling energy to the PDN when electricity prices are high. Second, to participate in frequency control reserve, which is needed for the PDN operator to ensure that the power supply and demand are constantly balanced. The BEB can supply the required additional energy or consume extra energy when there is a gap between the electricity demands and the supply. Some research studies have studied the supply of BEB transit systems using renewable energies. Ren et al. (2022) suggested a strategy to minimize the payback period of integrating rooftop PV panels and batteries for meeting the net-zero energy of the BEB transit system. Although it showed the economic and environmental benefits of deploying PV panels, it has disregarded the scheduling of the BEB transit system and the real charging demands required by the transit system and the PDN to be met.

Regardless of the extensive research on BEB scheduling and charging infrastructure, a comprehensive approach that integrates these aspects with the PDN's constraints and the intermittency of renewable energy sources remains elusive. This study addresses these challenges, seeking to bridge this gap for the integrated optimization of charging infrastructure planning and BEB scheduling, considering impacts on PDN. Particularly, we consider the complexities of the PDN and explore how renewable energy sources can offset the adverse effects of BEB charging demands on the PDN.

3. Problem description and modelling

3.1. Problem description

This research considers a bus transit system with a pre-scheduled timetable, spanning from the first service trip in the morning to the last in the evening, covering all service trips. The buses are parked at one or more depots, where they can be charged. Additionally, there is an option for en-route recharging at designated bus stations with chargers between service trips. Chargers at depots and bus stations are connected to a PDN (referred to as*charging demands*) as shown in Fig. 1. The PDN also caters to its regular consumers, referred to as *electrical demands* in this study. The charging demands are massive loads for the PDN in some peak hours, while the transportation sector should ensure that the charging demands do not endanger the safe and efficient operation of the PDN. RES generation and electrical storage system can be installed at PDN node $b \in \mathcal{B}_r$, where $\mathcal{B}_r \subset \mathcal{B}$, to supply the required charging demands of BEB, while RESs and BESs are the assets of the transportation system (specifically bus transit system in this work). Nevertheless, the bus transit system can supply its required charging demands by purchasing electricity from the PDN and procuring electricity from the RESs and BESs. In summary, this study aims to address the following key aspects.

- Planning the optimal location and size of charging infrastructure to ensure that it does not compromise the safe operation of the PDN.
- Planning the optimal number of buses required to adhere to the pre-scheduled timetable with cost minimization of the electric bus system.
- Planning the optimal number of chargers to support the charging demands in both depot and bus stations. The term en-route charging refers to charging at bus stops located along the route where there is sufficient time for charging. Our optimization methodology allows possible charging at every bus stop. However, it should be noted that our case study only considers charging at the starting or ending bus stops or stations or depots after finishing a trip as the stopping time at the intermediate bus stops of a trip is very short (1–2 min) in our case study and we do not consider wireless charging at bus stops.

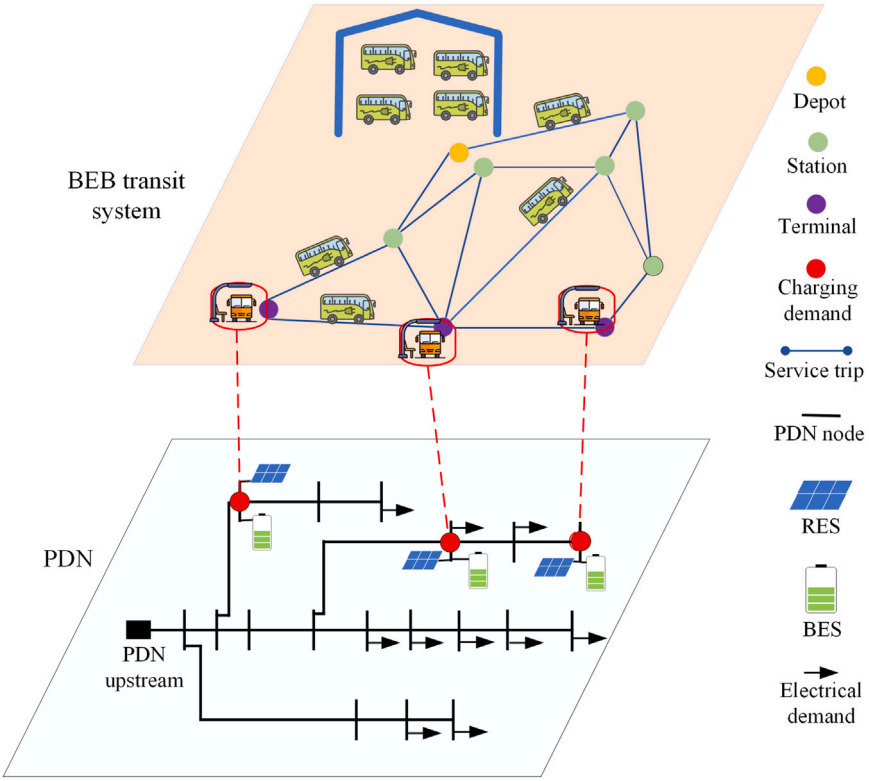

Fig. 1. Schematic of the proposed transit and power distribution network.

- Determining the optimal scheduling of BEB charging/discharging, considering PDN's technical limitations to prevent violations of voltage limits in PDN.
- Determining the optimal location and size of RESs and BESs to maintain PDN safety and minimize the cost of the electric bus system.

To achieve the aforementioned goals, we base our case study on the following assumptions.

- Each bus departs from the depot at the origin node in the morning for the first trip and returns to the depot at the destination in the evening after the last trip, and does not come back to the depot in the middle of the day to be recharged.
- BEBs can be recharged only in the depot and bus stations between trips, after completing a service trip, and before commencing the next. It is not allowed to be recharged during a service trip.
- This study focuses on urban electric bus systems around city areas and does not incorporate the long distances between cities. Therefore, we do not consider the situation that the range of electric bus is not enough for finishing a bus trip where mandatory charging during a trip is needed.
- Each bus leaves the depot in the morning with a near-full charge (more than 90% of its capacity), adhering to a minimum allowable charge level (more than 20% of its capacity).
- While the timetable remains fixed, the generation of RESs and electricity prices are subject to daily variations.
- It is assumed that the RESs and BESs can only be installed where BEB stations are coupled to the PDN.

We consider that the coupled system (BEB transit system and PDN) is operated within a time horizon $\mathcal{T}$. Serving the bus timetables calls for a very fine time discretization, with a timeslot duration of one minute, which adds to the problem's complexity. We define three main sets and three unions to propose our approach. Let $\mathcal{O}$ and $\mathcal{D}$ denote the sets of the first trip (from origin) and last trip (to destination) of all routes, which are located at a depot(s). The set of service trips is denoted by $\mathcal{S}$. Then, we define $\mathcal{OS} = \mathcal{O} \cup \mathcal{S}$, including all trips except the last trip, $\mathcal{SD} = \mathcal{D} \cup \mathcal{S}$ to include all service trips except the first trip, and $\mathcal{I} = \mathcal{O} \cup \mathcal{S} \cup \mathcal{D}$ to consider all trips. In the following subsections, we first present the objective function. Second, we provide the model for charging infrastructure planning and scheduling. Then, we give the model of the PDN and RES planning. The charging infrastructure is connected to the PDN, and it imposes an additional load on the PDN. On account of the large number of variables in the proposed model, we summarize the meaning and notations for variables in the nomenclature at the end of this paper to reduce redundancy.

3.2. Objective function

The objective function aims at minimizing the total infrastructure and operation cost of electric bus systems. The infrastructure cost is a one-time cost, including the costs of procuring buses, charging infrastructure planning, and RES-BES systems. The operation cost includes the electricity that is purchased from the PDN to supply charging demands. The decision variables are the number of buses required to serve trips, location and size of the chargers, scheduling of buses (how to serve the trips), charging scheduling (where to charge and how to charge (time and charged energy)), location and size of the RES and BES. The operation decision variables are related to the deployment of the installed equipment, i.e., the energy generation and charging/discharging of the BES and the electricity purchasing from the PDN. To address the aforementioned decision variables, first, we provide the objective function model to calculate the total planning and operation costs. Second, we provide the model of charging infrastructure planning, which gives the required capacity and location of the chargers. Then, we present the charging schedule to realize the required charging during trips and in the depot. Afterwards, the PDN model gives the technical constraints of the PDN coupled with the BEB transit system to analyse the effect of the BEB transit system on the PDN. Then, the last subsection presents the model of RES-BES planning to obtain the required RES-BES capacity to maintain the safe operation of the PDN.

(1) Infrastructure cost: The infrastructure cost is proposed as

$$\begin{aligned} IC = & \sum_{i\in S}\sum_{o\in\mathcal{O}} \rho x_{oi} + \\ & \sum_{i\in D,k\in\mathcal{K}} \mathrm{I}_{i,k}^{Ch,Sel} C_k^{Ch} + \sum_{n\in\mathcal{N}_b^d,k\in\mathcal{K}} \mathrm{N}_{n,k}^{Ch} C_k^{Ch} I_n + \\ & \sum_{b\in\mathcal{B}_r} [PV_b^{\mathrm{Cap}} C^{\mathrm{PV}} + \overline{\mathrm{E}}_b C^{\mathrm{BES}}]. \end{aligned} \tag{1}$$

The first term indicates the cost of procuring and maintenance of buses to serve the planned trips to fulfil the timetables of bus routes. The cost of procuring a bus is included when $x_{oi} = 1$, which means a bus departs the depot from the origin node. The second row in the equation denotes the cost of procuring and maintenance of chargers in the depot and bus stops. The cost of en-route chargers is imposed when its binary variable (I_n) is one. The third row shows the capital cost (procurement and maintenance) of installing RES-BES (herein PV), which is calculated with respect to the capacity (or size) of the PV panel.

(2) Operation cost: The operation cost (OC) stems from the required electricity purchased from the PDN to supply the charging demands.

$$OC = \sum_{t\in\mathcal{T}}\sum_{b\in\mathcal{B}_r}\sum_{w\in\mathcal{W}} \pi_w \rho_t^{\mathrm{M}} p_{wtb}^{\mathrm{DN2B}}. \tag{2}$$

The operation cost includes the purchase of time-of-use electricity with PDN.

(3) Total cost: The infrastructure cost is a one-time cost, while the operation cost is a time-dependent cost. Therefore, one of them should be scaled to unify both costs. We use the present value factor to scale the infrastructure cost (Bahmani-Firouzi and Azizipanah-Abarghooee, 2014).

$$TC = P^{\mathrm{VF}} \times IC + OC, \tag{3}$$

where P^{VF} is the present value factor, which is calculated as,

$$P^{\mathrm{VF}} = \frac{N^{\mathrm{Day}}}{365}\left[\frac{ir(1+ir)^{\mathrm{ny}}}{(1+ir)^{\mathrm{ny}-1}}\right], \tag{4}$$

where the interest rate ir for financing the installed RES, BES, and changing infrastructure, the number of years (ny), and the number of days (N^{Day}) are considered to calculate currency/day cost.

3.3. Charging infrastructure planning constraints

In our model, it is assumed that buses are charged only between two successive trips, namely after finishing a trip i and before starting the next trip j. The feasible charging time period is defined to incorporate the feasible time for charging between the trips (the time period when can charge the bus between trip i and trip j), such that the travel time of deadhead trips should be subtracted from the obtain the feasible time period. We call it *feasible charging time period* for the rest of the paper.

$$p_{injt}^{\mathrm{Ter}} \le x_{ij} p^{\mathrm{CMax}}, \quad \forall i,j \in S, i \ne j, t \in [\overline{u}_i + \tau_i^{\mathrm{DH}}, \underline{u}_j - \tau_j^{\mathrm{DH}}], n \in \mathcal{N}_b, \tag{5}$$

$$p_{injt}^{\mathrm{Ter}} \le \delta_{in} p^{\mathrm{CMax}}, \quad \forall i,j \in S, i \ne j, t \in [\overline{u}_i + \tau_i^{\mathrm{DH}}, \underline{u}_j - \tau_j^{\mathrm{DH}}], n \in \mathcal{N}_b, \tag{6}$$

$$p_{injt}^{\mathrm{Ter}} = 0, \quad \forall \{i,j \in \mathcal{O}\} \cup \{i,j \in \mathcal{D}\} \cup \{i = j\} \cup \{t \notin [\overline{u}_i + \tau_i^{\mathrm{DH}}, \underline{u}_j - \tau_j^{\mathrm{DH}}]\}, n \in \mathcal{N}_b, \tag{7}$$

$$\delta_{in} \le x_{ij} I_n, \quad \forall i,j \in S, i \ne j, n \in \mathcal{N}_b, \tag{8}$$

$$\sum_{i,j\in S} p_{injt}^{\mathrm{Ter}} \le p_n^{\mathrm{TMax}}, \quad \forall t \in \mathcal{T}, n \in \mathcal{N}_b, \tag{9}$$

$$p_n^{\mathrm{TMax}} \le M I_n, \quad \forall t \in \mathcal{T}, n \in \mathcal{N}_b. \tag{10}$$

Here, Eq. (5) indicates the power of charging that is restricted by the maximum charging power that can be received by the bus. This limitation can come from either BEB or the PDN for the sake of safety. It is important to note that t is a discrete index representing minute-based time intervals. In our methodology, we discretize the time into one-minute intervals. The binary variable δ_{in} is 1 or 0 when the bus is being charged or not being charged in Eq. (6), respectively. Eqs. (5) and (6) are valid only when the feasible charging time period is given. Otherwise, the charge received by the bus is 0 based on Eq. (7). The charging variable is only equal to 1 if there are trips i and j as indicated in Eq. (8). The maximum amount of power of charge indicates the required capacity of the charging station in Eq. (9). It also indicates that the maximum charging infrastructure capacity is a function of the transportation node n connected to the PDN, without additional restrictions on the location of the charging infrastructure. In other words, each charging station is a potential candidate for en-route charging. The binary variable I_n indicates whether a charging station is installed at node n of transit system and enforces this limitation in Eq. (10).

Additionally, a charging station can be installed at buses depot if needed. However, charging at the depot is only scheduled after the last trip in the evening (back to the depot) or before the first trip in the morning (before departure from the depot).

$$p_{ijt}^{\mathrm{Dep}} \le x_{ij} p^{\mathrm{CMax}}, \quad \forall i \in \mathcal{S}, j \in \mathcal{D}, i \ne j, t \in \{[\underline{u}_1 - \tau_i^{\mathrm{O2S}}] \cup [\overline{u}_j + \tau_{ij}^{\mathrm{S2D}}]\}, \tag{11}$$

$$p_{ijt}^{\mathrm{Dep}} = 0, \quad \forall\{i \notin \mathcal{S}\} \cup \{j \notin \mathcal{D}\} \cup \{i = j\} \cup \{t \notin \{[\underline{u}_1 - \tau_i^{\mathrm{O2S}}] \cup [\overline{u}_j + \tau_{ij}^{\mathrm{S2D}}]\}\}, \tag{12}$$

$$\sum_{i,j \in \mathcal{S}} p_{ijt}^{\mathrm{Dep}} \le p_n^{\mathrm{DMax}}, \quad \forall t \in \mathcal{T}, n \in \mathcal{N}_b^d. \tag{13}$$

It is assumed that before starting the first trip of a day, the buses should be charged enough to meet the maximum limit of the state of charge (e.g., 90% of its capacity) (Hu et al., 2022). Therefore, the depot is mostly used to prepare the charge of the buses before starting the first trip in the morning. τ_i^{O2S} and τ_{ij}^{S2D} denote the travel time of the deadhead trip from the depot to the station for the first trip i and from the station of the last service trip to the depot, respectively. The received charge at the depot is restricted to the maximum allowable in Eq. (11). In case of any violation in the feasible charging time period, p_{ijt}^{Dep} is equal to zero in Eq. (12). The required capacity of charging infrastructure is determined through Eq. (13).

3.4. Number and type of chargers

The chargers can be installed in depots and bus stations (en-route). Chargers in the depots should charge BEBs to a fully charged state (or near fully charged, as specified), while en-route chargers provide enough energy for BEBs to complete their daily trips. Since the time intervals for en-route charging are very short, typically just a few minutes between trips, the main purpose of en-route charging is to support the BEBs in completing their trips rather than ensuring a fully charged state. Therefore, it should be ensured that the BEBs that arrive at bus stations within a short time period and need electricity, can be plugged in. We define an integer variable $\mathrm{N}_{n,k}^{Ch}$ to represent the number of type k chargers installed at bus station n (en-route). Eq. (14) ensures that the installed chargers can meet the maximum power requirements for all BEBs. Eqs. (15) and (16) guarantee that there are enough chargers for each individual BEB arriving at the bus stations, where the binary variable δ_{in} maps the bus stations to trips.

$$p_n^{\mathrm{TMax}} \le \sum_{k \in \mathcal{K}} \mathrm{N}_{n,k}^{Ch} \mathrm{P}_k^{Ch,\max}, \quad \forall n \in \mathcal{N}_b. \tag{14}$$

$$\sum_{i \in \mathcal{S}} x_{ij} \delta_{in} \le \sum_{k \in \mathcal{K}} \mathrm{N}_{n,k}^{Ch}, \quad \forall n \in \mathcal{N}_b, j \in \mathcal{S}, i \ne j. \tag{15}$$

$$p_{injt}^{\mathrm{Ter}} \le \delta_{in} M, \quad \forall i, j \in \mathcal{S}, n \in \mathcal{N}_b, t \in [\overline{u}_i + \tau_i^{\mathrm{DH}}, \underline{u}_j - \tau_j^{\mathrm{DH}}]. \tag{16}$$

Similarly, the required number of chargers in the depot to support the charging demands depends on the energy received by each BEB within the given time period. Compared to en-route charging, the charging demands in the depot are met over longer periods, with all BEBs needing to be plugged in after their last trip in the depot. Thus, the last trip of each BEB serves as an index to track which BEBs go to the depot. To manage this, we define a dynamic set $\mathcal{S}^{Dyn}$, indicating the subset of last trips that end at the depot ($\mathcal{S}^{Dyn} \subset \mathcal{S}$). Each index in this dynamic set corresponds to a trip that concludes at the depot. That is, if $x_{ij} = 1, \forall i \in \mathcal{S}, j \in \mathcal{D}$, then $\mathcal{S}^{Dyn}$ = yes. Essentially, the index of the last trip can be used to track the trips and BEBs simultaneously. Additionally, we define a binary variable $\mathrm{I}_{j,i,k}^{Ch}$ to assign BEB j to charger i of type k. Eqs. (17)–(21) determine the required number of chargers in the depot. The total energy of charging demands in the depot for all BEBs is constrained by the capacity and number of chargers within the available charging time (after the last and before the first trips) as shown in (17). The power supplied to each BEB is similarly limited by the capacity of the charger as indicated in (18). The power received by all BEBs should also be restricted to ensure the capacity of chargers is not exceeded when multiple BEBs are plugged in simultaneously, as stated in (19). Eq. (20) indicates that one single BEB cannot be plugged into two chargers simultaneously. Finally, (21) specifies the required number and types of chargers.

$$e^{\max} \le \sum_{i \in \mathcal{S}^{Dyn}} \mathrm{I}_{i,k}^{Ch,Sel} \mathrm{P}_k^{Ch,\max} \frac{(u^{\mathrm{L}} - u^{\mathrm{F}})}{|\mathcal{T}|}, \tag{17}$$

$$p^{\text{Dep}}_{j,i\in D,t} \le \sum_{i\in S^{Dyn},k\in\mathcal{K}} \mathrm{I}^{Ch}_{j,i,k}\mathrm{P}^{Ch,\max}_{k}, \quad \forall j \in S^{Dyn}, t \in \mathcal{T}, \tag{18}$$

$$\sum_{j\in S^{Dyn}} p^{\text{Dep}}_{j,i,t} \le \sum_{i\in S^{Dyn},k\in\mathcal{K}} \mathrm{I}^{Ch,Sel}_{i,k}\mathrm{P}^{Ch,\max}_{k}, \quad \forall i \in \mathcal{D}, t \in \mathcal{T}, \tag{19}$$

$$\sum_{i\in S^{Dyn},k\in\mathcal{K}} \mathrm{I}^{Ch}_{j,i,k} = 1 \quad \forall j \in S^{Dyn}, t \in \mathcal{T}, \tag{20}$$

$$\mathrm{I}^{Ch,Sel}_{i,k} = \mathrm{I}^{Ch}_{j,i,k} \quad \forall i,j \in S^{Dyn}, k \in \mathcal{K}, \tag{21}$$

3.5. Energy constraints of battery electric bus

Each bus begins the daily operation in the morning and returns to the depot after the last trip in the evening. These buses are recharged en route between the trips, thereby replenishing their energy. Energy consumption occurs during service trips (i.e. from the starting station to the ending station of a service trip), the trips from the depot to the starting station for the first service trip, the return from the ending station last trip to the depot, and any deadhead trips required for going other charging points for connecting to chargers. It is essential that the energy levels of the batteries in BEBs at all times adhere to their maximum capacity constraints. The following equations represent the constraints of energy level in the batteries:

$$e^{\text{Ter}}_{inj} = \frac{1}{|\mathcal{T}|}\sum_{t\in\mathcal{T}} p^{\text{Ter}}_{injt}, \quad \forall i,j \in S, n \in \mathcal{N}_b, \tag{22}$$

$$e^{\text{Dep}}_{ij} = \frac{1}{|\mathcal{T}|}\sum_{t\in\mathcal{T}} p^{\text{Dep}}_{ijt}, \quad \forall i \in S, j \in \mathcal{D}. \tag{23}$$

The energy that comes from the power distribution network, en route, and in the depot are given in Eqs. (22) and (23), respectively.

It is assumed that the buses are nearly fully charged, with a predetermined amount, when they depart the depot at the origin node. Therefore, Eq. (24) indicates this matter as

$$q_{oi} = x_{oi}\overline{\lambda}Q, \quad \forall i \in S, o \in \mathcal{O}. \tag{24}$$

We define two variables for the energy in batteries. $\tilde{q}_i$ shows the remaining energy level in the battery after finishing trip i. q_{ij} represents the energy level after finishing trip i and exactly before starting trip j. Accordingly, there are three places involving q_{ij}. In Eq. (25), when the buses depart the origin and after the first trip i, the remaining energy does not exceed its upper limit, subtracting the consumed energy of the deadhead trip (from the depot to trip i), and the energy consumed during trip i (c^{SL}_i). Second, in two successive trips, Eq. (26) concerns the amount of battery energy after finishing trip i, and trip j is the next trip. Please note there is a possibility to recharge the battery between two consecutive trips en route. Third, when all service trips are finished, the buses return to the depot. Eq. (27) declares the energy in batteries required for a deadhead trip to the depot after the last trip. The three constraints are valid when there is a connection between the trips ($x_{ij} = 1$); if not, they are converted to obvious constraints (He et al., 2023).

$$\tilde{q}_i \le (q_{oi} - c^{\text{O2S}}_{oi} - c^{\text{SL}}_i)x_{oi} + \overline{\lambda}Q(1 - x_{oi}), \quad \forall i \in S, o \in \mathcal{O}, \tag{25}$$

$$\tilde{q}_j \le (\tilde{q}_i + e^{\text{Ter}}_{inj} - c^{\text{ST}}_{ij} - c^{\text{SL}}_j)x_{ij} + \overline{\lambda}Q(1 - x_{ij}), \quad \forall i,j \in S, i \ne j, n \in \mathcal{N}_b, \tag{26}$$

$$q_{ij} \le (\tilde{q}_i - c^{\text{S2D}}_{ij})x_{ij} + \overline{\lambda}Q(1 - x_{ij}), \quad \forall i \in S, j \in \mathcal{D}. \tag{27}$$

The BEB should be recharged at the depot after all service trips to a predetermined energy level to get ready for the next day's service trips based on (28). The energy stored in BEBs at the depot cannot violate its capacity range as restricted in (29).

$$(q_{ij} + e^{\text{Dep}}_{ij})x_{ij} \ge \overline{\lambda}Qx_{ij}, \quad \forall i \in S, j \in \mathcal{D}, \tag{28}$$

$$\underline{\lambda}Qx_{ij} \le q_{ij}x_{ij} \le \overline{\lambda}Qx_{ij}, \quad \forall i \in S, j \in \mathcal{D}. \tag{29}$$

Similarly, the energy of the BEBs should respect its range when the bus finishes the first trip, when the buses leave the depot at the origin in Eq. (30). The energy level during the trips and after recharging Eq. (31) and energy consumption for the next deadhead trip for the next service trip j in Eq. (32) are restricted by the upper and lower battery capacity bounds.

$$\underline{\lambda}Qx_{oi} \le (q_{oi} - c^{\text{O2S}}_{oi} - c^{\text{SL}}_i)x_{oi} \le \overline{\lambda}Qx_{oi}, \quad \forall i \in S, o \in \mathcal{O}, \tag{30}$$

$$\underline{\lambda}Qx_{ij} \le (\tilde{q}_i + e^{\text{Ter}}_{inj})x_{ij} \le \overline{\lambda}Qx_{ij}, \quad \forall i,j \in S, n \in \mathcal{N}_b, \tag{31}$$

$$\underline{\lambda}Qx_{ij} \le (\tilde{q}_i + e^{\text{Ter}}_{inj} - c^{\text{ST}}_{ij} - c^{\text{SL}}_j)x_{ij} \le \overline{\lambda}Qx_{ij}, \quad \forall i,j \in S, n \in \mathcal{N}_b. \tag{32}$$

The bus operation schedule consists of a timetable with a number of service trips, and each service trip is performed by one bus. To capture this feature, x_{ij} is defined as a binary variable, where $x_{ij} = 1$, if trip i is connected to trip j, namely trip j is immediately after trip i (Duan et al., 2023). Eq. (33) indicates that each service trip is exactly covered once. Constraint (34) shows the bus flow conservation constraint of the network. The conservation bus flow constraint ensures that the inflow of a trip should be equal to its outflow (Li et al., 2021). Trip j should be served exactly after trip i, without any overlap in time, considering the deadhead trip time in (35). Dual variables are given after the colons.

$$\sum_{k\in\mathcal{K}}\sum_{j\in\mathcal{SD},i\neq j} x_{ij} = 1, \quad \forall i \in \mathcal{S} : \varrho_i, \tag{33}$$

$$\sum_{i\in\mathcal{SD},i\neq j} x_{ji} - \sum_{i\in\mathcal{OS},i\neq j} x_{ij} = 0, \quad \forall j \in \mathcal{S} : \varpi_j, \tag{34}$$

$$\overline{u}_i + \tau_i + \tau_i^{\mathrm{DH}} \leq \underline{u}_j + M(1 - x_{ij}), \quad \forall i, j \in \mathcal{S}, i \neq j : \vartheta_{ij}. \tag{35}$$

3.6. Power flow model

We consider a radial PDN where a node $b \in \mathcal{B}$ denotes the index of a unique parent node ζ_b and a set $\mathcal{C}_b$ of children nodes. The active and reactive power balance equations for a node $b \in \mathcal{B}$ are given by the power flow model (Wang et al., 2016; Baran and Wu, 1989) and below equations.

$$P_{\zeta_b b,w,t} = \sum_{c\in\mathcal{C}_b} P_{bc,t,w} - \mathrm{r}_{\zeta_b \mathrm{b}} \frac{(P^{\mathrm{P}}_{b,w,t})^2 + (Q^{\mathrm{P}}_{b,w,t})^2}{(V_{b,w,t})^2} - p^{\mathrm{P}}_{b,w,t}, \quad \forall b \in \mathcal{B}, w \in \mathcal{W}, t \in \mathcal{T}, \tag{36}$$

$$Q_{\zeta_b b,w,t} = \sum_{c\in\mathcal{C}_b} Q_{bc,t,w} - \mathrm{x}_{\zeta_b \mathrm{b}} \frac{(P^{\mathrm{P}}_{b,w,t})^2 + (Q^{\mathrm{P}}_{b,w,t})^2}{(V_{b,w,t})^2} - q^{\mathrm{P}}_{b,w,t}, \forall b \in \mathcal{B}, w \in \mathcal{W}, t \in \mathcal{T}, \tag{37}$$

where $P_{\zeta_b b,w,t}$ ($Q_{\zeta_b b,w,t}$) is the active (reactive) power flowing in line (ζ_b, b). Parameter $\mathrm{r}_{\zeta_b \mathrm{b}}$ ($\mathrm{x}_{\zeta_b \mathrm{b}}$) is the line's resistance (reactance). $V_{b,w,t}$ is the node's voltage. $p^{\mathrm{P}}_{b,w,t}$ ($q^{\mathrm{P}}_{b,w,t}$) is the node's net power injection, which is defined by the node's RES generation $P^{\mathrm{RES}}_{b,w,t}$, and charging demand $P^{\mathrm{BEB}}_{b,w,t}$. The power demand $D^{\mathrm{P}}_{b,t}$ indicates the input demands of the PDN nodes which can include various types of demands e.g., residential, commercial, industrial, etc. . The formulation reads

$$p^{\mathrm{P}}_{b,w,t} = D^{\mathrm{P}}_{b,t} - p^{m}_{wtb} - P^{\mathrm{RES,D}}_{b,w,t} - p^{\mathrm{Dch}}_{wtb} + P^{\mathrm{BEB}}_{b,w,t} \quad \forall b \in \mathcal{B}, w \in \mathcal{W}, t \in \mathcal{T}, \tag{38}$$

while the reactive power injection is defined in a similar manner as

$$q^{\mathrm{P}}_{b,w,t} = D^{\mathrm{Q}}_{b,t} - Q^{\mathrm{CAP}}_{b,t} \quad \forall b \in \mathcal{B}, s \in \mathcal{W}, t \in \mathcal{T}, \tag{39}$$

with $Q^{\mathrm{CAP}}_{b,t}$ denoting the reactive power injection of the node's capacitor bank. The voltage drop between two adjacent nodes is governed by

$$V^2_{\zeta_b,w,t} = V^2_{b,w,t} - 2(\mathrm{r}_{\zeta_b \mathrm{b}} P_{\zeta_b b,w,t} + \mathrm{x}_{\zeta_b \mathrm{b}} Q_{\zeta_b b,w,t}) + (\mathrm{r}^2_{\zeta_b \mathrm{b}} + \mathrm{x}^2_{\zeta_b \mathrm{b}}) \frac{(P^{\mathrm{P}}_{b,w,t})^2 + (Q^{\mathrm{P}}_{b,w,t})^2}{V^2_{b,w,t}}, \quad \forall b \in \mathcal{B}, w \in \mathcal{W}, t \in \mathcal{T}, \tag{40}$$

and the safe operation of the PDN requires that all voltages remain within safe bounds.

$$\underline{V} \leq V_{b,w,t} \leq \overline{V} \quad \forall b \in \mathcal{B}, w \in \mathcal{W}, t \in \mathcal{T}. \tag{41}$$

The charging demands can be supplied through RES directly, discharging of the BES, and purchasing electricity from the PDN as given in Eq. (42)

$$P^{\mathrm{RES,D}}_{b,w,t} + p^{\mathrm{Dch}}_{wtb} + p^{\mathrm{DN2B}}_{wtb} \geq \sum_{i,j\in\mathcal{S}} p^{\mathrm{Ter}}_{injt} + p^{\mathrm{Dep}}_{ijt} \quad \forall b \in \mathcal{B}_r, n \in \mathcal{N}_b, w \in \mathcal{W}, t \in \mathcal{T}. \tag{42}$$

A linear derivation of the adopted power flow is used in order to reduce the complexity level by disregarding the high-order terms in Eqs. (36), (37), and (40). The effectiveness of the presented linear version is verified in the relevant studies by Wang et al. (2016), Baran and Wu (1989). The linearized power flow model is formulated as

$$P_{\zeta_b b,w,t} = \sum_{c\in\mathcal{C}_b} P_{bc,t,w} - D^{\mathrm{P}}_{b,t} + P^{\mathrm{RES,D}}_{b,w,t} + p^{\mathrm{Dch}}_{wtb} + p^{m}_{wtb} - P^{\mathrm{BEB}}_{bwt}, \quad \forall b \in \mathcal{B}, w \in \mathcal{W}, t \in \mathcal{T} \quad : \mu_{wtb} \tag{43}$$

$$Q_{\zeta_b b,w,t} = \sum_{c\in\mathcal{C}_b} Q_{bc,t,w} - D^{\mathrm{Q}}_{b,t} + Q^{\mathrm{CAP}}_{b,t}, \quad \forall b \in \mathcal{B}, w \in \mathcal{W}, t \in \mathcal{T} \quad : \sigma_{wtb}, \tag{44}$$

$$V_{\zeta_b,w,t} = V_{b,w,t} - (\mathrm{r}_{\zeta_b \mathrm{b}} P_{\zeta_b b,w,t} + \mathrm{x}_{\zeta_b \mathrm{b}} Q_{\zeta_b b,w,t}), \quad \forall b \in \mathcal{B}, w \in \mathcal{W}, t \in \mathcal{T} \quad : \kappa_{wtb}. \tag{45}$$

3.7. RES planning constraints

The imposed charging demands by BEBs cannot jeopardize the safe and normal operation of the PDN. Hence, the strategy is to compensate the charging demands from BEBs by RES for two purposes: first, to keep the operation of PDN safe and second, to increase the energy generation by clean sources. Here, we consider PV generation as an RES in this study, while it can be extended to other RESs (e.g. wind turbines).

$$P^{\mathrm{RES}}_{b,w,t} \le P^{PV,Max}_{wt} PV^{\mathrm{Cap}}_{b}, \quad \forall b \in \mathcal{N}_b, w \in \mathcal{W}, t \in \mathcal{T} \quad : \iota_{wtb} \tag{46}$$

$$P^{\mathrm{RES}}_{b,w,t} = P^{\mathrm{RES,D}}_{b,w,t} + p^{\mathrm{Ch}}_{wtb}, \quad \forall b \in \mathcal{B}_r, w \in \mathcal{W}, t \in \mathcal{T} \quad : \varepsilon_{bwt} \tag{47}$$

$$P^{\mathrm{RES}}_{b,w,t} \le M \cdot I^{RES}_{b}, \quad \forall b \in \mathcal{B}_r, w \in \mathcal{W}, t \in \mathcal{T} \quad : \xi_{wtb} \tag{48}$$

$$PV^{\mathrm{Cap}}_{b} \le PV^{\mathrm{CapMax}}_{b}, \quad \forall b \in \mathcal{B}_r \quad : \bar{\iota}_{wtb} \tag{49}$$

Each PDN node b can be a candidate for the installation of a RES-BES system, including PV panels and a BES bank in the BEB stations or depot ($b \in \mathcal{B}_r$). The RES generation $P^{\mathrm{RES}}_{b,w,t}$ cannot exceed its capacity and the potential of power generation (which depends on solar irradiation) in Eq. (46). The generated electricity by the RES can go through electrical demands or be stored in the BES as given in Eq. (47). A RES-BES system can only be installed in bus stations and depots as indicated in Eq. (48). The installed PV capacities are limited considering land use in (49). The land use limitations for PV panels are restricted to various constraints and considerations related to the amount, type, and quality of land required for installing PV systems such as land area requirements, land type limitations, topographic and geographic constraints, and land ownership and regulatory constraints. However, in this study, we only investigate the land area requirements. Interested readers are referred to Ong et al. (2013) for further details.

3.8. Planning of battery electric storage

The BES, as a flexible resource frequently used in PDNs, is considered to facilitate the operation of PDNs. The BES at PDN node b has the state of charge e^{BES}_{wtb} indicated as

$$e^{\mathrm{BES}}_{wtb} = e^{\mathrm{BES}}_{w,t-1,b} - \frac{1}{|\mathcal{T}|\eta^{\mathrm{d}}_{b}} p^{\mathrm{Dch}}_{wtb} + \frac{1}{|\mathcal{T}|}\eta^{\mathrm{c}}_{b} p^{\mathrm{Ch}}_{wtb}, \quad \forall b \in \mathcal{B}_r, t \in \mathcal{T}, w \in \mathcal{W}, \quad : \upsilon_{wtb}. \tag{50}$$

The state of charge of the BES is restricted in (51) by its upper and lower bounds as

$$\underline{\Theta}\overline{\mathrm{E}}_{b} \le e^{\mathrm{BES}}_{wtb} \le \overline{\Theta\mathrm{E}}_{b}, \quad \forall b \in \mathcal{B}_r, t \in \mathcal{T}, w \in \mathcal{W}, \quad : \underline{\vartheta}_{wtb}, \overline{\vartheta}_{wtb}. \tag{51}$$

The upper bound $\overline{\mathrm{E}}_{b}$ is derived through the optimization problem. Besides, Eqs. (52) and (53) indicate either charging or discharging of the BES at the same time

$$p^{\mathrm{Ch}}_{wtb} \le M\mathcal{I}^{Ch}_{wtb}, \quad \forall b \in \mathcal{B}_r, t \in \mathcal{T}, w \in \mathcal{W}, \quad : Y^{Ch}_{wtb}, \tag{52}$$

$$p^{\mathrm{Dch}}_{wtb} \le M(1 - \mathcal{I}^{Ch}_{wtb}), \quad \forall b \in \mathcal{B}_r, t \in \mathcal{T}, w \in \mathcal{W}, \quad : Y^{Dch}_{wtb}. \tag{53}$$

We use the binary variable $\mathcal{I}^{Ch}_{wtb}$ to ensure either charge or discharge simultaneously. Charging/discharging is only allowed on bus stations where RES can be installed, as in Eqs. (54) and (55)

$$p^{\mathrm{Ch}}_{wtb} \le \overline{\Psi\mathrm{E}}_{b}, \quad \forall b \in \mathcal{B}_r, t \in \mathcal{T}, w \in \mathcal{W}, \quad : \phi^{Ch}_{wtb}, \tag{54}$$

$$p^{\mathrm{Dch}}_{wtb} \le \overline{\Psi\mathrm{E}}_{b}, \quad \forall b \in \mathcal{B}_r, t \in \mathcal{T}, w \in \mathcal{W}, \quad : \phi^{Dch}_{wtb}. \tag{55}$$

The initial state of charge of the BES is indicated in Eq. (56)

$$e^{\mathrm{BES}}_{w,t0,b} = SOC^{ini}_{b}, \quad \forall b \in \mathcal{B}_r, t \in \mathcal{T}, w \in \mathcal{W}, \quad : \eta_{wb}. \tag{56}$$

4. Solution methodology

The proposed model exhibits a notable complexity, primarily attributable to the extensive array of variables and the presence of nonlinear constraints. A significant challenge in solving this model arises from the intricacies associated with the bus scheduling variable x_{ij}. This variable introduces nonlinearity into Eqs. (25)–(32). To effectively address the nonlinearity and alleviate the computational burden, we have adopted a strategic approach by partitioning the solution process into two distinct phases: a master problem and a subproblem. This bifurcation is executed by applying Benders Decomposition, a technique that enables a more manageable and efficient problem-solving framework.

4.1. Subproblem

The scheduling of buses, and RES-BES (location and size) are optimized in the subproblem. The objective function of the subproblem is to minimize the total cost, including purchasing buses, the cost of installing RES-BES, and the operation cost of BEBs (i.e., electricity purchase costs).

$$UB = P^{\text{VF-Bus}} \sum_{i\in S}\sum_{o\in O} \rho x_{oi} + \sum_{b\in B_r}\left[P^{\text{VF-PV}} \cdot PV_b^{\text{Cap}} C^{\text{PV}} + P^{\text{VF-BES}} \cdot \overline{\text{E}}_b C^{\text{BES}}\right] + \sum_{t\in T}\sum_{b\in B_r}\sum_{w\in W} \pi_w \rho_t^{\text{M}} p_{wtb}^{\text{DN2B}}. \tag{57}$$

The values of $\hat{p}_{injt}^{\text{Ter}}$, $\hat{p}_{ijt}^{\text{Dep}}$ are derived from the master problem and their values are included in the power flow Eq. (43) as $P_{bwt}^{\text{BEB}} = \hat{p}_{injt}^{\text{Ter}} + \hat{p}_{ijt}^{\text{Dep}}$. The objective of the subproblem is the upper bound (UB) of the problem. The subproblem is subject to Eqs. (8), (33)–(35), (41) and (43)–(56). Since Eq. (8) is nonlinear, so it is reformulated as

$$\hat{\delta}_{ij} \le I_n, \quad \forall ij \in S, i \ne j, n \in \mathcal{N}_b, : \varphi_{ijn}, \tag{58}$$

$$\hat{\delta}_{ij} \le x_{ij}, \quad \forall ij \in S, i \ne j, : \varsigma_{ij}, \tag{59}$$

where the dual variables are provided after the colons. The charger deployment $\hat{\delta}_{ij}$ is also taken from the master problem.

4.2. Master problem

The master problem addresses the charging schedule and deployment of chargers (whether to use the installed charger (δ_{in})). The lower bound of the decomposed problem (LB) is obtained by solving the master problem by adding the following objective function α and the constraints of the LB as

$$\min \ \alpha \tag{60}$$

$$\begin{aligned}\alpha \ge & \sum_{i\in S}\hat{o}_i + \sum_{i,j\in S, i\ne j}\left[\hat{\vartheta}_{ij} - \hat{\vartheta}_{ji}\overline{u}_i + \hat{\vartheta}_{ij}(\tau_i + \tau_i^{\text{DH}} - M)\right] + \\ & \sum_{i,j\in S}\hat{\varsigma}_{ij}\delta_{in} + \sum_{i,j\in S}\sum_{v\in}\hat{\varphi}_{ijv}\delta_{in} + \\ & \sum_{i,j\in S}\sum_{n\in\mathcal{N}_b}\sum_{w\in W}\sum_{t\in T}\sum_{b\in B}[\hat{p}_{injt}^{\text{Ter}} + \hat{p}_{ijt}^{\text{Dep}}]\mu_{wtb} + \\ & \sum_{w\in W}\sum_{t\in T}\sum_{b\in B}\left[D_{bt}^P\mu_{wtb} + D_{bt}^Q\sigma_{wtb} + MY_{wtb}^{Dch}\right] + \sum_{w\in W}\sum_{b\in B} SOC_b^{ini}\eta_{wb} + \\ & P^{\text{VF-Ch}}\left[\sum_{i\in D,k\in K}\text{I}_{i,k}^{Ch,Sel}C_k^{Ch} + \sum_{n\in\mathcal{N}_b,k\in K}\text{N}_{n,k}^{Ch}C_k^{Ch}\hat{I}_n\right] + \sum_{t\in T}\sum_{b\in B}\sum_{w\in W}\text{Pen}_{wtb}.\end{aligned} \tag{61}$$

Here, α is the lower bound of the problem, and it consists of two parts. The first part comes from the dual objective function of the subproblem, where the variables of the subproblem are fixed inputs in the master determined through ε–$\hat{\varepsilon}$. The second part stems from the main objective function of the problem. The objective function is constrained to Eqs. (5)–(7), Eqs. (9)–(32) and Eq. (61). A penalty term Pen_{wtb} is used in the objective function to ensure the feasibility of the constraint Eq. (42) updated in Eq. (62)

$$\hat{P}_{wtb}^{\text{RES,D}} + \hat{P}_{wtb}^{\text{Dch}} + \hat{P}_{wtb}^{\text{DN2B}} + \text{Pen}_{wtb} \ge \sum_{i,j\in S} p_{injt}^{\text{Ter}} + p_{ijt}^{\text{Dep}} \quad \forall b \in B_r, n \in \mathcal{N}_b, w \in W, t \in T. \tag{62}$$

4.3. Alternative feasibility cut

There is always the possibility of an unbounded solution when a problem is decomposed into two separate problems. Therefore, it is necessary to consider alternative solutions. To be more specific, the subproblem may be unbounded, given the solution of the master problem. Here, we consider a feasibility cut as an alternative for the iterations in which the master problem is unbounded. The dual subproblem is used in the form of the extreme ray to create a mathematical objective function to obtain an alternative feasible cut (Taşkin, 2011).

$$\begin{aligned}\max & \sum_{i\in S}\varrho_i + \sum_{i,j\in S, i\ne j}\left[\vartheta_{ij} - \vartheta_{ji}\overline{u}_i + \vartheta_{ij}(\tau_i + \tau_i^{\text{DH}} - M)\right] + \sum_{i,j\in S}\varsigma_{ij}\hat{\delta_{in}} + \\ & \sum_{i,j\in S}\sum_{n\in\mathcal{N}_b}\varphi_{ijn}\hat{\delta_{in}} + \sum_{i,j\in S}\sum_{n\in\mathcal{N}_b}\sum_{w\in W}\sum_{t\in T}\sum_{b\in B}[\hat{p}_{injt}^{\text{Ter}} + \hat{p}_{ijt}^{\text{Dep}}]\mu_{wtb} + \\ & \sum_{w\in W}\sum_{t\in T}\sum_{b\in B}\left[D_{bt}^P\mu_{wtb} + D_{bt}^Q\sigma_{wtb} + MY_{wtb}^{Dch}\right] + \sum_{w\in W}\sum_{b\in B} SOC_b^{ini}\eta_{wb},\end{aligned} \tag{63}$$

subject to

$$x_{ij}: \quad \varrho_i + \varpi_i - \varpi_j - M(\vartheta_{ij} + \varsigma_{ij} + \sum_{n\in\mathcal{N}_b} \varphi_{ijn}) \le 0, \quad \forall i,j \in \mathcal{S}, i \ne j, n \in \mathcal{N}_b, \tag{64}$$

$$I_n: \quad \sum_{i,j\in\mathcal{S}} \varphi_{ijn} \le 0, \quad \forall n \in \mathcal{N}_b, \tag{65}$$

$$P_{bwt}: \quad \mu_{wt,b-1} - \mu_{wtb} - r_b \le 0, \quad \forall b \in \mathcal{B}, w \in \mathcal{W}, t \in \mathcal{T}, \tag{66}$$

$$p^{\mathrm{Dch}}_{wtb}: \quad \mu_{wtb} + \frac{\upsilon_{wtb}}{|\mathcal{T}|\eta^d_b} + Y^{Dch}_{wtb} + \phi^{Dch}_{wtb} \le 0, \quad \forall b \in \mathcal{B}, w \in \mathcal{W}, t \in \mathcal{T}, \tag{67}$$

$$P^{\mathrm{RES,D}}_{b,w,t}: \quad \mu_{wtb} - \varepsilon_{wtb} \le 0, \quad \forall b \in \mathcal{B}, w \in \mathcal{W}, t \in \mathcal{T}, \tag{68}$$

$$p^m_{bwt}: \quad \mu_{wtb} \le 0, \quad \forall b \in \mathcal{B}, w \in \mathcal{W}, t \in \mathcal{T}, \tag{69}$$

$$Q_{bwt}: \quad \sigma_{wt,b-1} - \sigma_{wtb} - x_b \le 0, \quad \forall b \in \mathcal{B}, w \in \mathcal{W}, t \in \mathcal{T}, \tag{70}$$

$$q^m_{bwt}: \quad \sigma_{wtb} \le 0, \quad \forall b \in \mathcal{B}, w \in \mathcal{W}, t \in \mathcal{T}, \tag{71}$$

$$V_{b,w,t}: \quad \kappa_{wt,b-1} - \kappa_{wtb} + \overline{\kappa}_{wtb} + \underline{\kappa}_{wtb} \le 0, \quad \forall b \in \mathcal{B}, w \in \mathcal{W}, t \in \mathcal{T}, \tag{72}$$

$$P^{\mathrm{RES}}_{b,w,t}: \quad \xi_{wtb} + \iota_{wtb} + \bar{\iota}_{wtb} + \varepsilon_{wtb} \le 0, \quad \forall b \in \mathcal{B}, w \in \mathcal{W}, t \in \mathcal{T}, \tag{73}$$

$$I^{RES}_b: \quad \sum_{w\in\mathcal{W}} \sum_{t\in\mathcal{T}} M\xi_{wtb} \le 0, \quad \forall b \in \mathcal{B}_r, \tag{74}$$

$$e^{\mathrm{BES}}_{wtb}: \quad \upsilon_{wtb} - \upsilon_{w,t-1,b} + \overline{\vartheta}_{wtb} + \underline{\vartheta}_{wtb} + \eta_{wb} \le 0, \quad \forall b \in \mathcal{B}, w \in \mathcal{W}, t \in \mathcal{T}, \tag{75}$$

$$p^{\mathrm{Ch}}_{wtb}: \quad -\frac{\eta^{Ch}_b \upsilon_{wtb}}{|\mathcal{T}|} + Y^{Ch}_{wtb} + \phi^{Ch}_{wtb} - \varepsilon_{wtb} \le 0, \quad \forall b \in \mathcal{B}, w \in \mathcal{W}, t \in \mathcal{T}, \tag{76}$$

$$I^{Ch}_{wtb}: \quad MY^{Dch}_{wtb} - MY^{Ch}_{wtb} \le 0, \quad \forall b \in \mathcal{B}, w \in \mathcal{W}, t \in \mathcal{T}, \tag{77}$$

$$\overline{E}_b: \quad -\overline{\Theta\vartheta}_{wtb} - \underline{\Theta\vartheta}_{wtb} - \Psi\phi^{Ch}_{wtb} - \Psi\phi^{Dch}_{wtb} \le 0, \quad \forall b \in \mathcal{B}, w \in \mathcal{W}, t \in \mathcal{T}, \tag{78}$$

where the dual variables of (64) and (78) are given before the colon. For the aforementioned dual variables, $\mu_{wtb}, \sigma_{wtb}, \kappa_{wtb}, \varepsilon_{wtb}$, υ_{wtb} and η_{wb} are unlimited variables. $\overline{\kappa}_{wtb}, \xi_{wtb}, \iota_{wtb}, \overline{\vartheta}_{wtb}, Y^{Ch}_{wtb}, Y^{Dch}_{wtb}, \phi^{Ch}_{wtb}$ and ϕ^{Dch}_{wtb} are non-positive variables. Besides, $\underline{\kappa}_{wtb}$ and ϑ_{wtb} are non-negative variables. In order to better comprehend the steps of the decomposition methods, the flowchart of the proposed approach is given in Fig. 2 to elaborate on how to connect different steps.

5. Numerical experiments and results

5.1. Case study

The proposed approach has been applied to a real BEB transit system in Skövde, Sweden. We have taken three routes from the center of the city to the north and northeast of the city. The separate timetable of each route can be found in Västtraffik (2023). The gathered timetable includes a total of 833 trips on the three routes mentioned. The first trip starts at 04:50, and the last trip ends at 23:58. There are five candidate bus stations to install chargers and one depot, as shown in Fig. 3. The length of the routes #1, #2 and #3 are 9.1, 14, 6.4 km, respectively. The bus stations are mapped to the 33-node PDN with a medium voltage level (12.66 kV), as shown in Fig. 4. In a medium-voltage system, low-voltage consumers are connected to a transformer, which then links them to the medium-voltage system. The initial electrical active and reactive demands of the PDN are 3700 kW and 1800 kVar, respectively. The characteristics of the demands and impedance of the PDN are taken from Najafi et al. (2020), wherein it is assumed that the demands on different nodes follow a consistent pattern for simplicity. Respecting the optimization, we merged two trips if the time gap between two trips is not enough for a bus to charge (less than 5 min). As a result, the number of bus trips decreases to 316 trips. Additionally, according to the given timetable, sufficient charging time is available only at the end of routes in our case study after merging trips. However, this does not affect the generality of the model. If adequate charging time is available between two consecutive trips in any given case study, they are considered separately (i.e., not merged) to account for the possibility of en-route charging.

In the case study, we conducted the optimization for 24 h a day. The electricity prices at different times are referred to Nordpool (2023) by taking the prices of area pricing #3, Sweden, which includes Skövde. Fig. 5 shows the electricity prices. For the sake of reducing the computational complexity of the problem, we have considered each 2-minute interval as our sample time. Therefore,

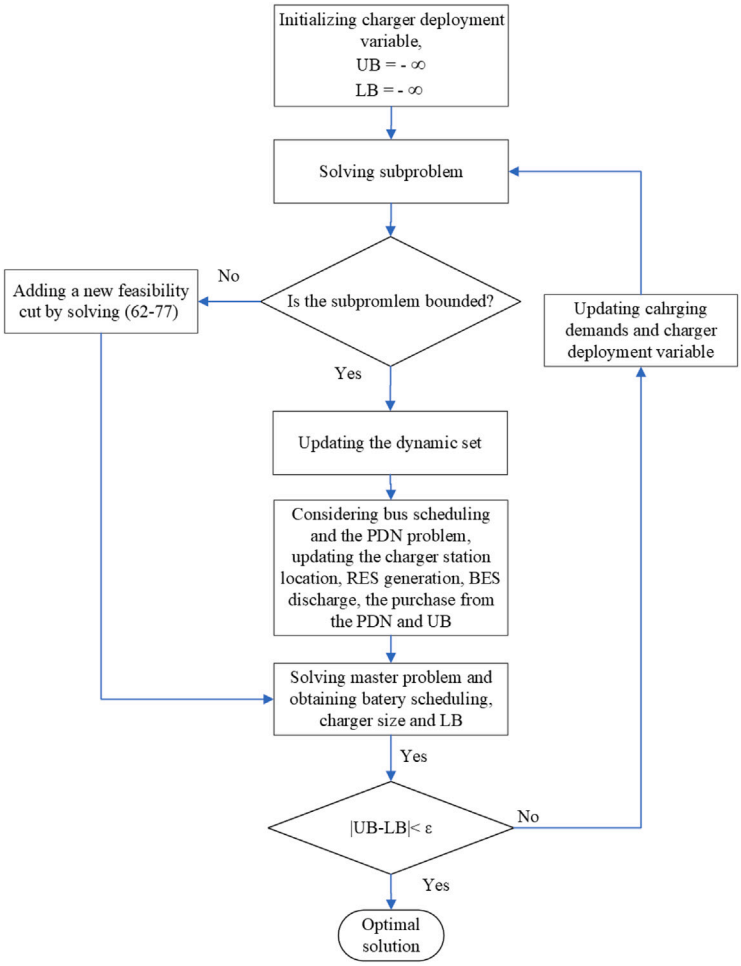

Fig. 2. Flowchart of the decomposition method.

there are 720 samples. The electricity generation of PV is uncertain due to several factors, such as solar radiation. We consider three scenarios to address the uncertainty in the electricity generation of PV. The normalized expected value of electricity generation of PV is provided in Fig. 5. The scenarios are generated with the given expected value, including a 15% standard deviation at each hour using the normal distribution function. The electrical demand has the given total peak value of 3700 kW, and it changes hourly, developing the pattern given in Fig. 5. For instance, if one node has a peak value of 100 kW, then by applying the pattern of the demands, it can change from $0.792 \times 100 = 79.2$ kW to $1 \times 100 = 100$ kW. The lower and upper limits of voltage in the power grid for safe operations are 0.9 and 1.05 pu, respectively. The energy consumption per kilometer is assumed to be 1.67 kWh, and the average speed is 30 km/h. Based on the information from ABB (2024b), three types of slow chargers with capacities of 50 kW, 100 kW, and 150 kW, as well as three types of fast chargers with capacities of 300 kW, 450 kW, and 600 kW, are considered as potential candidates. The prices for these charger types are taken from European Automobile Manufacturers' Association (ACEA) (2024), with values of €28,000, €50,000, €60,000, €74,000, €111,000, and €125,000, respectively.

The BEBs are hematogenous and the minimum and maximum levels of the energy of the BEBs are 20% and 90%, respectively. The range of energy levels for the BES are assumed to be 10% and 90%. The cost of each bus with the capacity of 350 kWh is €500000 considering procurement and maintenance. The type of electric bus can drive around 200 km in normal situations. The PV and BES capital costs (procurement and maintenance) are assumed to be 1250 and €250 per kW. The lifetimes of the batteries, chargers, and PV panels are assumed to be six, fifteen, and thirty years, respectively (Ufine Battery, 2024; ABB, 2024a; U.S. Energy Information Administration (EIA), 2024). Additionally, the maximum possible capacity for PV installations, based on the available land, is assumed to be 1000 kW. The maximum electrical demand is positioned at node #25 of the PDN, where the demand is 420 kW. The maximum charger power is also 600 kW. Hence, we assume that the maximum charging capability of a station is 900 kW for BEBs considering other electrical demands and candidate chargers power. However, it can change in different cases. The numeric case studies are carried out on a Ci5 laptop with 16 GB RAM. The proposed linear model has been formulated in GAMS and solved by CPLEX.

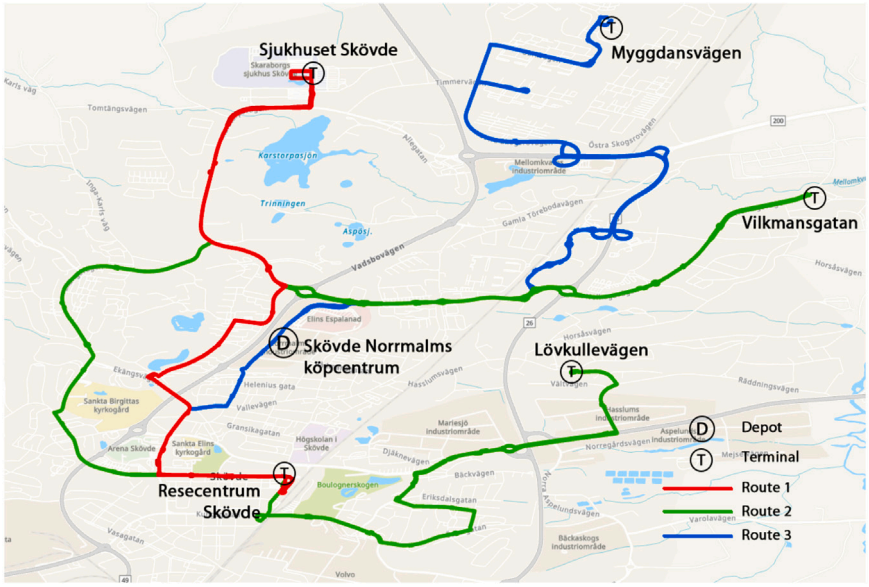

Fig. 3. Routes understudy in the city of Skövde.

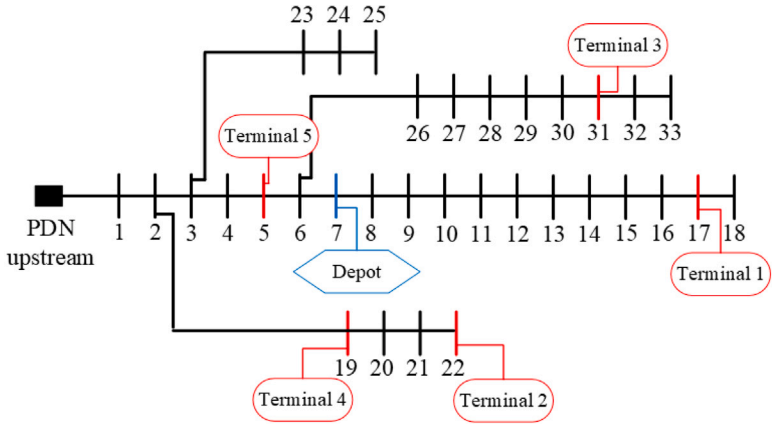

Fig. 4. Standard IEEE 33 nodes PDN test-case.

5.2. Results and discussion

The section presents the results of the case study for both the BEB transit system and the PDN by providing the optimal location and size for planning the infrastructure in both the transit system and the PDN, and investigating the impact of charging demands on the PDN.

Table 1 provides information on the installed capacity of chargers in the depot and bus stations after optimization.

As indicated by the results, a total charging capacity of 600 kW, 150 kW, and 900 kW is needed in bus stations #3, #4 and #5, respectively, while no charging capacity is required in bus stations #1 and #2. The charging capacities are provided by one charger with capacity of 600 kW in bus station #3, one charger with a capacity of 150 kW in bus station #4, and two chargers with the capacities of 300 kW and 600 kW at bus station 5. Table 2 gives the value of installed RES and BES capacities in candidate bus stations and depots. The top two highest PV capacities are installed on PDN nodes #17. Since PDN node #17 is located at the end of the longest PDN feeder (which has the highest voltage drop intrinsically), the high capacities of PV are deployed in this PDN node to support the charging demands from electric buses at these locations and mitigate the impacts of high charging demand from electric buses on the power grid. Capacities of 326 kW and 699 kW are also installed at nodes #5 and #7, corresponding to the locations of bus station #5 and the depot. The depot is near bus station #5, which has a charging infrastructure capacity of 900 kW. The PV and BES at nodes #5 and #7 can support both locations due to their proximity, thus mitigating any adverse impacts on the power grid at these two sites. It is important to consider the feasibility of installing high-capacity PV panels in urban areas, particularly in terms of the required land or roof space for their installation (e.g., the aforementioned 1000 kW capacity) (Jahangir et al., 2020).

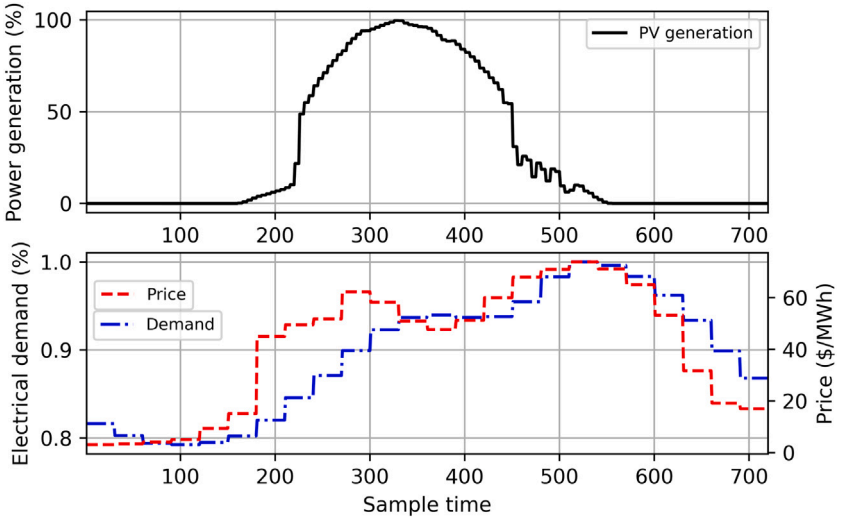

Fig. 5. Expected PV generations, PDN demands and electricity prices.

Table 1
Required charger capacities in different locations.

Location name	Installed place	Charger capacity (kW)	Number of chargers
Norrmalms	Depot	600	1
Myggdansvägen	bus station 1	0	0
Vilkmansgatan	bus station 2	0	0
Sjukhuset Skövde	bus station 3	600	1
L̀ovkullev'agen	bus station 4	150	1
Resecentrum Skövde	bus station 5	300, 600	1, 1

Table 2
Required PV and BES capacities.

Location (PDN node)	PV Capacity (kW)	BES capacity (kWh)
5	326	998
7	699	1292
17	1000	2217
31	296	1081

To calculate the required land for PV installation, we use the equation provided in Kermani et al. (2021), as follows:

$$PV_b^{\text{Cap}} = GHI \times \text{Area} \times \eta^{\text{PV}}, \tag{79}$$

where GHI is the global horizontal irradiation (W/m^2), Area is the total area m^2, and η^{PV} is the efficiency of the panels. Considering $GHI = 1000$, and $\eta^{\text{PV}} = 0.16$, given in Kermani et al. (2021), the total required area for the highest PV capacity in the bus stations (1000 kW), is 6250 m^2. Nevertheless, the high capacity of PVs may need some locations from that node to host the panels, e.g., malls, and buildings in addition to the provided lands on roofs in the bus stations.

The design of electricity transfer mechanism between PV and BES systems depends on the installed capacity of the sources. For small capacities, PV and BES systems are typically connected through DC-links by connecting to a low-voltage power grid. However, the PV and BES systems incorporated in this study are high-capacity sources (beyond 200 kw). Therefore, the assumed PDN is a medium-voltage test case designed to directly accommodate high-capacity PV systems and BES. Both PV and BES are directly connected to the PDN according to corresponding standards (Kermani et al., 2022). This means that electricity transfer between the PV, BES and PDN is facilitated through the PDN infrastructure, owing to the size of the sources (Kermani et al., 2022).

Table 3 summarizes the cost of charging infrastructure, PV, BES, bus, and the electricity purchased from the PDN to support the charging demand from BEBs. The highest cost is dedicated to procuring ten buses (€500000 each) to cover all routes and trips. It should be mentioned that the costs of BES, PV, charging infrastructure, and bus procurement are one-time costs, while the electricity purchase cost is a variable cost that is related to time.

Fig. 6 depicts the optimal scheduling of the buses to fulfil the trips for different routes. The total required number of buses is 10 to support the scheduled trips. As can be seen from the figure, a bus runs the trips for different routes to fully utilize each bus, satisfying the constraints from charging needs and spatial distributions of bus stations. For example, in the studied day, bus #2 covers 34 trips starting from trip #2 and ending with trip #314. bus #2 starts with running trips for route #2, covering routes #3

Table 3
Planning and scheduling costs.

Type	Cost (€)
BES	1 257 327
PV	2 901 460
Charging infrastructure	509 000
Bus	5 000 000
Electricity purchase from PDN	487

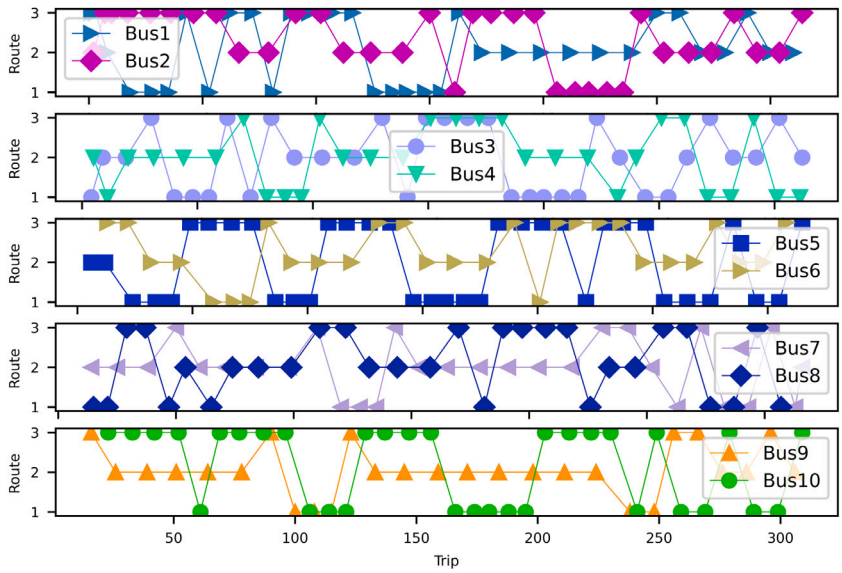

Fig. 6. Bus deployment to the trips and routes.

for the next seven trips, and then is back to cover trips in route #2 again. In the later hours, bus #2 covers some trips for route #1 as well. Similar patterns can be found for other buses. The scheduled bus trips may be different on different days, such as weekdays and weekends or different seasons. However, the proposed methodology is generic. For other scheduled trips on a different day, the proposed methodology can be used for scheduling optimization with only input changes.

The state of charge of buses #1 and #2 throughout the studied day are illustrated in Fig. 7. For brevity and clarity, we present results for buses #1 and #2 for demonstration, and the patterns of other buses are similar. The curve in the figure shows the changes in the energy level of buses #1 and #2 throughout the day, and the bars show the charged energy after a trip. For instance, bus #2 is charged after trips #102 and #161. After trip #102, a steep increase in the energy level curve indicates a higher charging power (here 120 kWh after trip #102). An interesting observation is that buses #1 and #2 are scheduled to reach their minimum state of charge by the end of their last trip. This occurs because the primary charging takes place at the depot with the lowest electricity prices, which leads to reduced electricity procurement costs.

Fig. 8 displays the state of charge of electric buses upon arrival at the depot, as well as the amount of energy received at the depot. It reveals that some of the BEBs i.e., buses #1, #2, #6, and #8 go to the depot with the minimum allowable charge and charge at the depot their maximum capacity. This behaviour is attributed to the low charging prices during midnight (see Fig. 5), which lead to reduced electricity procurement costs for BEBs. However, this trend is not uniform across all BEBs due to constraints on the number of available chargers and the associated costs of expanding the charging infrastructure. Fig. 9 illustrates the charging demands in the depot and bus stations to support the scheduled trips of BEBs during the day. There are high levels of charging demand in the middle of the day and during rush hours, which leads to a requirement for high-capacity charging infrastructure in some of the bus stations (see Table 1). During the time interval from 660 to 680, the charging demand peaks at 1500 kW, necessitating the use of the deployed capacities of 600 kW at bus stations #3 and #5, and 300 kW at bus station #5 (totalling 1500 kW). The charging capacity in the depot is effectively utilized during the early hours of the day to supply the required electricity for BEBs when electricity prices are at their lowest.

In addition to the electricity generated from RES, it is still necessary to purchase electricity from the PDN to charge the BEBs, during the beginning and ending hours of the day.

The initial PDN demands (such as residential and office electricity usage) excluding charging demands, are shown in Fig. 9 to provide a comprehensive understanding of the additional charging demands from BEBs, besides the baseline electricity demand from other sectors. The added charging demand from BEBs, particularly after time sample #600, reveals that the charging demands of BEBs reach up to 1500 kW, while the initial electricity demand from other sectors range between 3200–3400 kW. This highlights

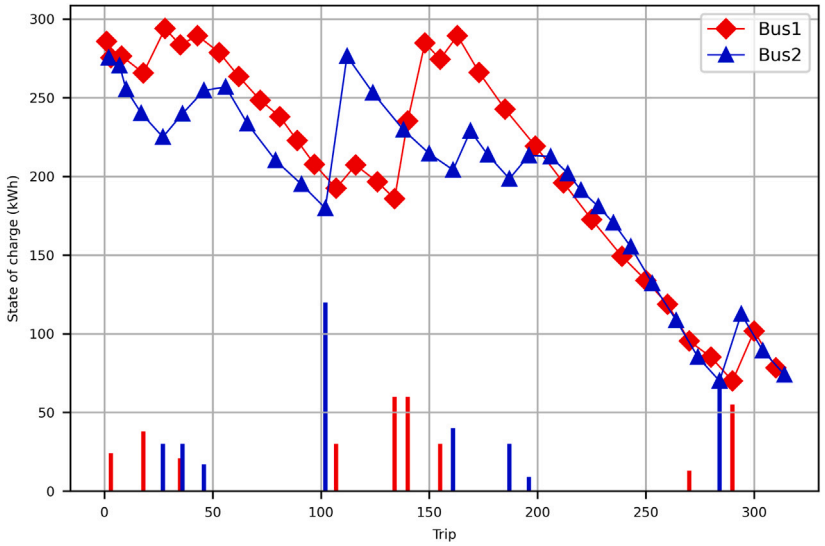

Fig. 7. Energy level of BEB during trips for bus #1 and bus #2 in the sample day of October.

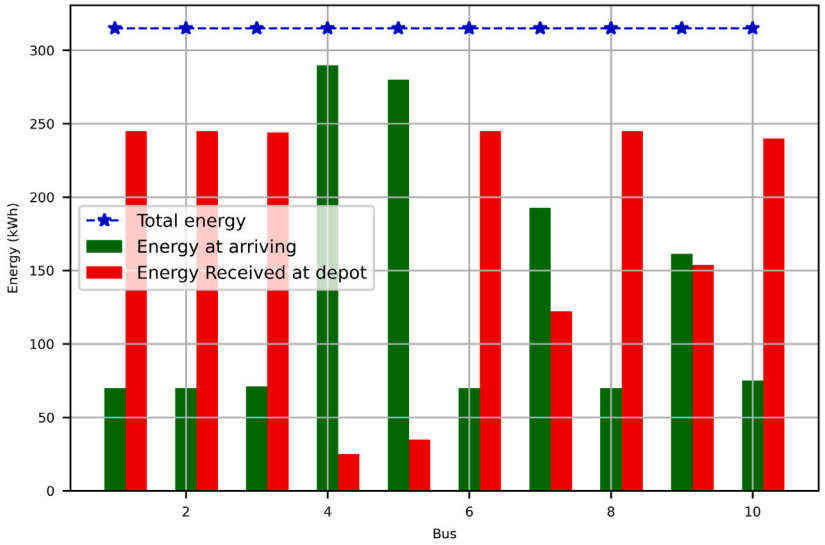

Fig. 8. Energy of BEBs arriving at the depot and received in the depot on the sample day of October.

the significant impact of charging demands of BEBs on the PDN. Our methodology leverages RES to compensate for the charging demand and then ensure the safe operation of PDN free from large overload or voltage drop. Fig. 10 shows the total electricity generated by the RES (i.e. PV), the difference between the charging demands and the electricity generated by the RES. The positive and negative values in the figure below mean more and less electricity generation from RES than the charging demand at a time frame, respectively. This figure also demonstrates the reason for deploying the BESs with PVs in the optimization model. When the electricity generation of the RESs is zero in the evening, there is still charging demand. In addition, sometimes, only a part of charging demands can be supplied by the PDN due to technical limitations of the PDN (e.g., overload on the PDN). Therefore, the BESs are required to store the electricity from RES during the daytime and use it to charge BEBs when it is needed during the night, which reduces the electricity bought from PDN.

Fig. 11 exhibits the total value of charging/discharging performed by the BES. The charging of BESs mostly happens when the PV generates electricity with solar radiation during the daytime. Stored electricity in BESs are used to satisfy charging demands in peak hours (i.e. discharging of BESs) in order to support the PDN (or BEB), which is correlated with the peak hours of the PDN electrical demands. For a better understanding, the charging and discharging from BESs are investigated in the PDN node #31 in Fig. 12. This node is located at the end of the PDN network (see Fig. 4), which is regarded as a critical PDN node. Therefore, a package of PV and BES is installed at this node. The electricity generated by the PV can be stored or transferred to the PDN directly.

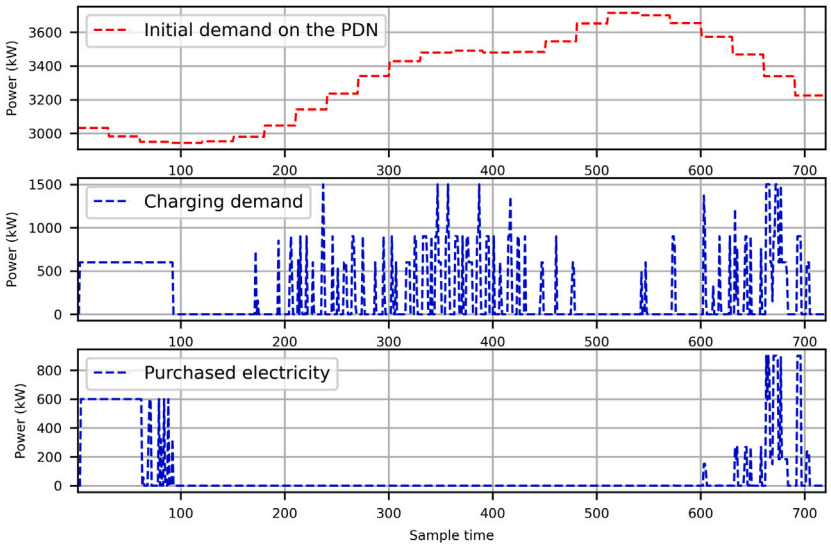

Fig. 9. Amount of power purchased from the upstream by the PDN and required charging demand in the sample day of October.

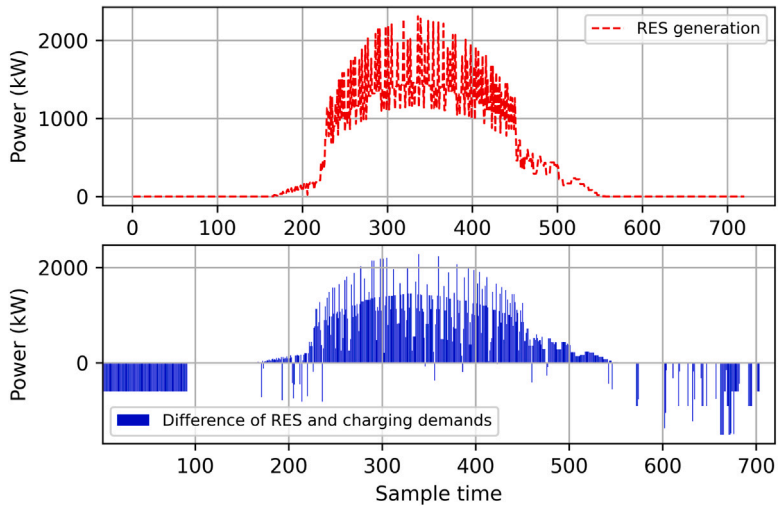

Fig. 10. Generated PV power and required electricity in the presence of RESs in the sample day of October.

The stored electricity in BESs is discharged when it is needed due to the charging demands, particularly, in the rush hours to support the massive charging demands after time sample #650. Both options of PV and BES discharge are used to charge BEBs at node #31.

Fig. 13 depicts the value of voltage in all PDN nodes. The PDN nodes 15–18 and 32–33 exhibit the lowest voltage while respecting the minimum value of 0.9 pu when RESs are considered. These nodes are the most critical nodes in the PDN. With disregarding the RESs and BESs in Fig. 13-b, the voltage violations occur in these PDN nodes, namely, the voltage falls below 0.9. Fig. 14 compares the minimum voltage of all nodes in the studies period under the situations of considering the RES with BES or not. It can be observed that without RES with BES, some PDN nodes fail to meet the constraints of the PDN in terms of a minimum voltage of 0.9 pu, where the voltage on PDN nodes 9–17 and 28–33 drop below 0.9 pu due to charging demand from BEBs. Referring to Fig. 11, a significant portion of the energy is discharged from BESs after time sample 500 when there are higher charging demands, and the discharging of BESs acting as the local electricity generation to help with avoiding an overload and voltage violation in PDN.

5.3. Computation complexity

This subsection elaborates on the complexity level of the proposed framework. The dimensions of problem are examined in terms of the number of binary, integer, and continuous variables, as well as the number of inequality and equality constraints in both the master and subproblem within a single iteration. The order of complexity is determined based on the dimensions of the sets in the

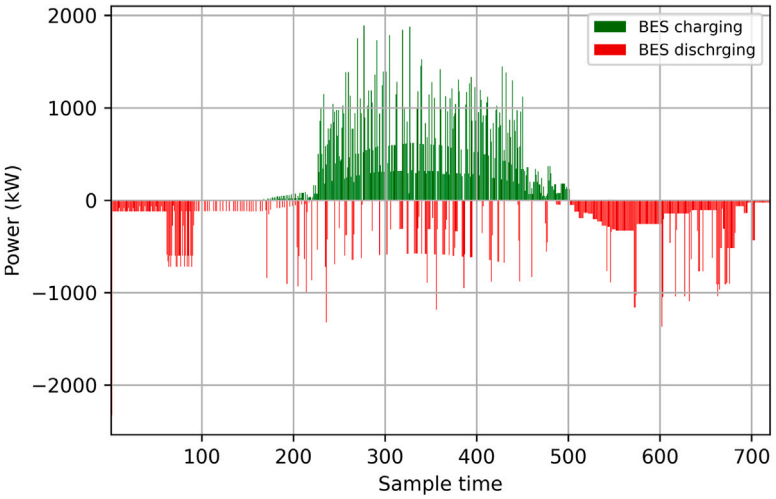

Fig. 11. Total charging/discharging of energy storage systems in the sample day of October.

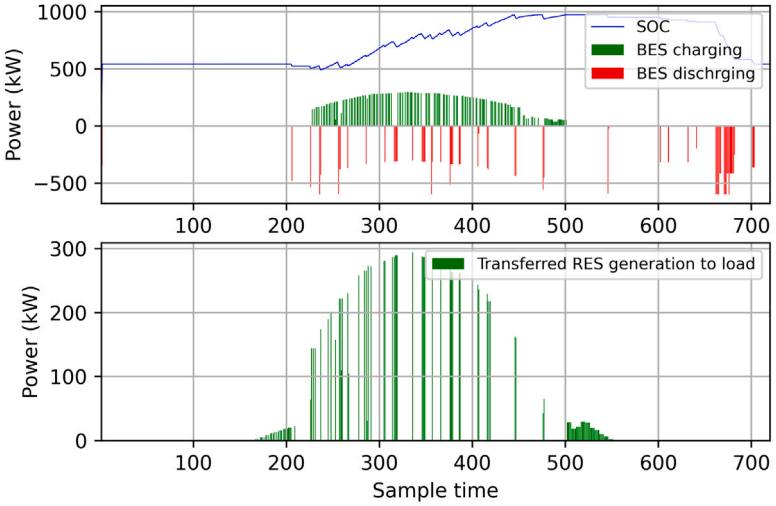

Fig. 12. Charging/discharging of energy storage systems in the sample day of October on PDN #31.

problem, as outlined in Table 4. Given the current dimensions of the sets, including $|\mathcal{T}| = 720, |S| = 316, |D| = |\mathcal{O}| = 1, |\mathcal{K}| = 6, |\mathcal{B}| = 33, |\mathcal{B}_r| = 6, |\mathcal{W}| = 3$ and $|\mathcal{N}| = 5$, the size of each row is derived. The current computational time is 64 min. It is evident that the problem size increases as the size of each set grows. This characteristic can be seen as one of the advantages of the proposed methodology, which can solve such complex problems by decomposing them. Despite the current large problem size, the proposed framework is capable of solving even larger problems with the use of more powerful computing resources. It is worth mentioning that our study focuses on long-term infrastructure planning and scheduling instead of real-time scheduling problems. The planning will not change very frequently in short periods, particularly the infrastructure. Therefore, it is not as time-critical in computation as other problems such as speed control and real-time scheduling.

6. Conclusion

This study proposes a novel framework for joint planning of charging infrastructure, charging scheduling and renewable energy resources coupled with the PDN. Special emphasis is put into holistic optimization of charging infrastructure planning, BEB scheduling and PDN integration, considering mutual interactions. Renewable energy resources including PV panels and BESs are utilized to mitigate excessive charging demand of BEBs and its adverse impacts on PDN. The optimal number of BEBs, the location and size of charging infrastructure, location and size of RES with BES, and BEB charging scheduling are jointly determined in the proposed framework. On account of the complexity of the problem, a decomposition method is proposed to linearize and reduce the computational burdens for finding solutions. A numerical case study based on three bus routes in the city of Skovde, Sweden

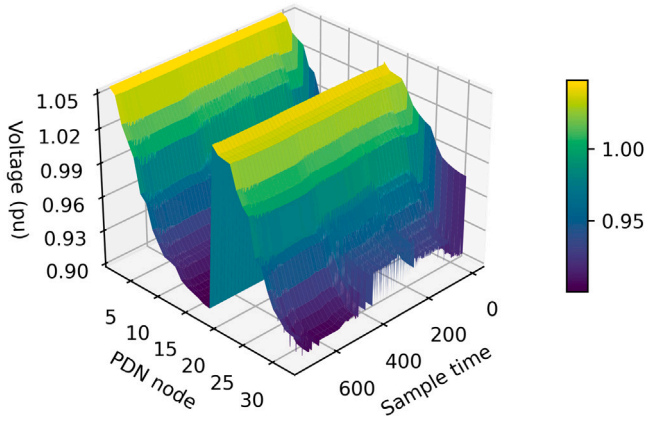

(a) Considering RESs

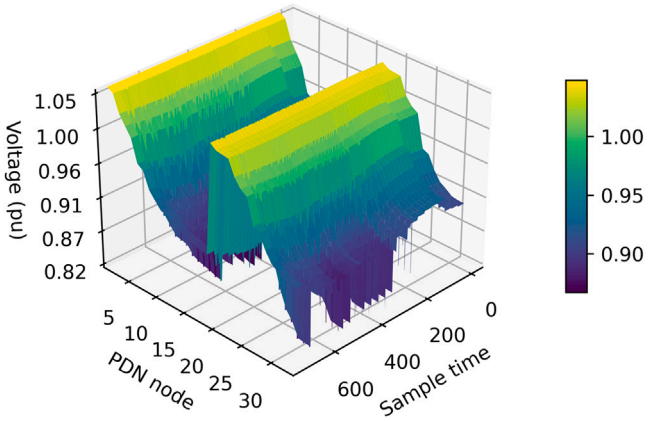

(b) Disregarding RESs

Fig. 13. Obtained voltage during the horizon for all PDN nodes in October.

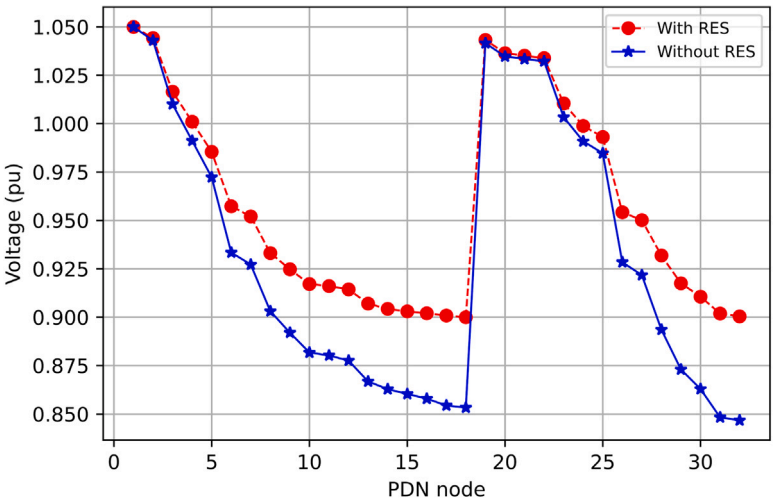

Fig. 14. Minimum obtained voltage during whole planning horizon.

Table 4
Computational complexity level of the master and subproblem.

	Type of #	Order of complexity	Current size
Master problem	# of binary variables	$\lvert\mathcal{N}\rvert + \lvert\mathcal{S}\rvert\lvert\mathcal{K}\rvert + \lvert\mathcal{S}\rvert^2\lvert\mathcal{K}\rvert$	601 037
	# of integer variables	$\lvert\mathcal{N}\rvert\lvert\mathcal{K}\rvert$	30
	# of continuous variables	$\lvert\mathcal{S}\rvert^2\lvert\mathcal{N}\rvert\lvert\mathcal{T}\rvert + 2\lvert\mathcal{N}\rvert + \lvert\mathcal{S}\rvert^2\lvert\mathcal{N}\rvert + 2\lvert\mathcal{S}\rvert^2 + 2\lvert\mathcal{S}\rvert + \lvert\mathcal{O}\rvert\lvert\mathcal{S}\rvert$	360 181 550
	# of equality constraints	$1 + 2\lvert\mathcal{S}\rvert^2\lvert\mathcal{N}\rvert + \lvert\mathcal{S}\rvert\lvert\mathcal{D}\rvert\lvert\mathcal{T}\rvert + \lvert\mathcal{S}\rvert\lvert\mathcal{T}\rvert + \lvert\mathcal{S}\rvert^2\lvert\mathcal{K}\rvert + \lvert\mathcal{S}\rvert\lvert\mathcal{D}\rvert + \lvert\mathcal{S}\rvert\lvert\mathcal{O}\rvert$	2 053 369
	# of inequality constraints	$8\lvert\mathcal{S}\rvert^2\lvert\mathcal{N}\rvert + 3\lvert\mathcal{T}\rvert\lvert\mathcal{N}\rvert + \lvert\mathcal{S}\rvert\lvert\mathcal{D}\rvert\lvert\mathcal{T}\rvert + \lvert\mathcal{N}\rvert + \lvert\mathcal{N}\rvert\lvert\mathcal{S}\rvert + \lvert\mathcal{S}\rvert^2\lvert\mathcal{N}\rvert\lvert\mathcal{T}\rvert + 2\lvert\mathcal{S}\rvert\lvert\mathcal{T}\rvert + \lvert\mathcal{D}\rvert\lvert\mathcal{T}\rvert + 3\lvert\mathcal{S}\rvert\lvert\mathcal{O}\rvert + 5\lvert\mathcal{S}\rvert\lvert\mathcal{D}\rvert + \lvert\mathcal{B}\rvert\lvert\mathcal{W}\rvert\lvert\mathcal{T}\rvert$	364 245 313
Subproblem	# of binary variables	$2\lvert\mathcal{S}\rvert^2 + \lvert\mathcal{B}\rvert + \lvert\mathcal{B}\rvert\lvert\mathcal{W}\rvert\lvert\mathcal{T}\rvert$	271 025
	# of continuous variables	$9\lvert\mathcal{B}\rvert\lvert\mathcal{W}\rvert\lvert\mathcal{T}\rvert + \lvert\mathcal{B}\rvert\lvert\mathcal{T}\rvert + \lvert\mathcal{B}\rvert$	665 313
	# of equality constraints	$2\lvert\mathcal{S}\rvert + 3\lvert\mathcal{B}_r\rvert\lvert\mathcal{W}\rvert\lvert\mathcal{T}\rvert + 3\lvert\mathcal{B}\rvert\lvert\mathcal{W}\rvert\lvert\mathcal{T}\rvert + \lvert\mathcal{B}\rvert$	253 385
	# of inequality constraints	$2\lvert\mathcal{S}\rvert^2 + 2\lvert\mathcal{B}_r\rvert\lvert\mathcal{W}\rvert\lvert\mathcal{T}\rvert + 2\lvert\mathcal{B}\rvert\lvert\mathcal{W}\rvert\lvert\mathcal{T}\rvert + 2\lvert\mathcal{S}\rvert^2\lvert\mathcal{N}\rvert$	1 366 752

is conducted using the proposed methodology. Results reveal that without RES, high charging demand from BEBs in some periods to fulfil running scheduling may result in violation of technical constraints of the PDN (more than 4% in this work), leading to large voltage drop and dangers for the safe operation of the PDN. The integration of RES with BESs in the BEB transit system can help to ensure the stability of the PDN while meeting the system's charging demands. This approach strategically allocates higher RES capacities to areas where the PDN is more vulnerable and the charging demand is more notable in some periods to mitigate the adverse impacts of excessive charging demand on PDN. The study also presents optimal charging infrastructure planning and efficient charging scheduling to reduce overall system cost.

Even though this research has contributed to the literature on joint optimization of charging infrastructure planning and charging scheduling coupled with renewable energy and power distribution networks, there are still some future perspectives and challenges to be addressed. First, the energy consumption of buses has been simplified within this study through a linear relation based solely on the driving distances as we focus on common scenarios for infrastructure planning and scheduling planning. A precise understanding of energy consumption necessitates data and consideration of the operational situation of BEBs in certain scenarios such as high passenger load and low temperature during winter. These aspects can affect the charging schedule strategies in the lower-level operational optimization based on more real-time and grained information. It is an interesting future perspective to refine energy consumption predictions influenced by various factors such as loading of passengers, weather conditions and temperatures, and propose a lower-level charging scheduling optimization based on more real-time input data. Second, the degradation cost of the batteries has been omitted in this work. However, the degradation cost is still a challenge for researchers due to the complex aspects of estimating the degradation cost. It will be challenging but interesting to combine a well-established degradation approach into our proposed analysis framework, promising a more comprehensive analysis. Moreover, our case study does not investigate the case of long-distance bus trips that exceed the range of common electric buses where mandatory charging during a trip is needed, as we focus on the electric bus systems in typical EU cities. It will be interesting future work to conduct another case study for between-city long-distance bus trips or coach trips if data are available. Last but not at least, the optimization problem is pretty complex due to a lot of nonlinearity. It is a promising and worthy future direction to further improve the optimization solution methods for such a complex optimization.

CRediT authorship contribution statement

Arsalan Najafi: Writing – review & editing, Writing – original draft, Project administration, Methodology, Investigation, Conceptualization. **Kun Gao:** Writing – review & editing, Validation, Supervision, Project administration, Methodology, Funding acquisition, Formal analysis, Conceptualization. **Omkar Parishwad:** Writing – review & editing, Writing – original draft, Investigation, Formal analysis. **Georgios Tsaousoglou:** Writing – review & editing, Writing – original draft, Formal analysis. **Sheng Jin:** Writing – review & editing, Validation, Formal analysis. **Wen Yi:** Writing – review & editing, Validation.

Declaration of competing interest

The authors declare that they have no known competing financial interests or personal relationships that could have appeared to influence the work reported in this paper.

Acknowledgements

The research is funded by JPI Urban Europe and Energimyndigheten (e-MATS, P2023-00029) and supported by Area of Advance Transport at Chalmers University of Technology. Any opinions, findings, conclusions or recommendations expressed in this paper are those of the authors and do not necessarily reflect the sponsors' views.

References

ABB, 2024a. Document ID 9AKK108468A1794. URL: https://search.abb.com/library/Download.aspx?DocumentID=9AKK108468A1794. (Accessed 02 December 2024).

ABB, 2024b. Pantograph up. https://new.abb.com/ev-charging/pantograph-up. (Accessed 25 July 2024).

Al-Saadi, M., Bhattacharyya, S., Tichelen, P.V., Mathes, M., Käsgen, J., Van Mierlo, J., Berecibar, M., 2022. Impact on the power grid caused via ultra-fast charging technologies of the electric buses fleet. Energies 15 (4), http://dx.doi.org/10.3390/en15041424, URL: https://www.mdpi.com/1996-1073/15/4/1424.

An, K., 2020. Battery electric bus infrastructure planning under demand uncertainty. Transp. Res. Part C: Emerg. Technol. 111, 572–587. http://dx.doi.org/10.1016/j.trc.2020.01.009, URL: https://www.sciencedirect.com/science/article/pii/S0968090X18314578.

Avishan, F., Yanıkoğlu, İ., Alwesabi, Y., 2023. Electric bus fleet scheduling under travel time and energy consumption uncertainty. Transp. Res. Part C: Emerg. Technol. 156, 104357. http://dx.doi.org/10.1016/j.trc.2023.104357, URL: https://www.sciencedirect.com/science/article/pii/S0968090X23003479.

Bahmani-Firouzi, B., Azizipanah-Abarghooee, R., 2014. Optimal sizing of battery energy storage for micro-grid operation management using a new improved bat algorithm. Int. J. Electr. Power Energy Syst. 56, 42–54. http://dx.doi.org/10.1016/j.ijepes.2013.10.019, URL: https://www.sciencedirect.com/science/article/pii/S0142061513004365.

Baran, M., Wu, F., 1989. Network reconfiguration in distribution systems for loss reduction and load balancing. IEEE Trans. Power Deliv. 4 (2), 1401–1407. http://dx.doi.org/10.1109/61.25627.

Basma, H., Haddad, M., Mansour, C., Nemer, M., Stabat, P., 2021. Assessing the charging load of battery electric bus fleet for different types of charging infrastructure. In: 2021 IEEE Transportation Electrification Conference & Expo. ITEC, pp. 887–892. http://dx.doi.org/10.1109/ITEC51675.2021.9490119.

Chen, Z., Yin, Y., Song, Z., 2018. A cost-competitiveness analysis of charging infrastructure for electric bus operations. Transp. Res. Part C: Emerg. Technol. 93, 351–366. http://dx.doi.org/10.1016/j.trc.2018.06.006, URL: https://www.sciencedirect.com/science/article/pii/S0968090X18308465.

Cui, S., Gao, K., Yu, B., Ma, Z., Najafi, A., 2023. Joint optimal vehicle and recharging scheduling for mixed bus fleets under limited chargers. Transp. Res. Part E: Logist. Transp. Rev. 180, 103335. http://dx.doi.org/10.1016/j.tre.2023.103335, URL: https://www.sciencedirect.com/science/article/pii/S136655452300323X.

Dong, G., Witlox, F., Bie, Y., 2024. Decentralizing e-bus charging infrastructure deployment leads to economic and environmental benefits. Commun. Transp. Res. 4, 100139. http://dx.doi.org/10.1016/j.commtr.2024.100139, URL: https://www.sciencedirect.com/science/article/pii/S2772424724000222.

Duan, M., Liao, F., Qi, G., Guan, W., 2023. Integrated optimization of electric bus scheduling and charging planning incorporating flexible charging and timetable shifting strategies. Transp. Res. Part C: Emerg. Technol. 152, 104175. http://dx.doi.org/10.1016/j.trc.2023.104175, URL: https://www.sciencedirect.com/science/article/pii/S0968090X2300164X.

El-Ela, A.A.A., El-Seheimy, R.A., Shaheen, A.M., Wahbi, W.A., Mouwafi, M.T., 2021. PV and battery energy storage integration in distribution networks using equilibrium algorithm. J. Energy Storage 42, 103041. http://dx.doi.org/10.1016/j.est.2021.103041, URL: https://www.sciencedirect.com/science/article/pii/S2352152X21007507.

El-Taweel, N.A., Farag, H.E.Z., Barai, G., Zeineldin, H., Al-Durra, A., El-Saadany, E.F., 2022. A systematic approach for design and analysis of electrified public bus transit fleets. IEEE Syst. J. 16 (2), 2989–3000. http://dx.doi.org/10.1109/JSYST.2021.3114271.

European Automobile Manufacturers' Association (ACEA), 2024. ACEA - European automobile manufacturers' association. URL: https://www.acea.auto/. (Accessed 26 July 2024).

Fei, F., Sun, W., Iacobucci, R., Schmöcker, J.-D., 2023. Exploring the profitability of using electric bus fleets for transport and power grid services. Transp. Res. Part C: Emerg. Technol. 149, 104060. http://dx.doi.org/10.1016/j.trc.2023.104060, URL: https://www.sciencedirect.com/science/article/pii/S0968090X23000499.

Gairola, P., Nezamuddin, N., 2023. Optimization framework for integrated battery electric bus planning and charging scheduling. Transp. Res. Part D: Transp. Environ. 118, 103697. http://dx.doi.org/10.1016/j.trd.2023.103697, URL: https://www.sciencedirect.com/science/article/pii/S1361920923000949.

Guo, J., Ding, Z., Yu, K., Tang, F., 2021. Optimal electric bus fleet charging scheduling considering passenger flow. In: 2021 IEEE/IAS Industrial and Commercial Power System Asia. I&CPS Asia, pp. 420–424. http://dx.doi.org/10.1109/ICPSAsia52756.2021.9621632.

Hache, E., Palle, A., 2019. Renewable energy source integration into power networks, research trends and policy implications: A bibliometric and research actors survey analysis. Energy Policy 124, 23–35. http://dx.doi.org/10.1016/j.enpol.2018.09.036, URL: https://www.sciencedirect.com/science/article/pii/S0301421518306499.

He, Y., Liu, Z., Song, Z., 2020. Optimal charging scheduling and management for a fast-charging battery electric bus system. Transp. Res. Part E: Logist. Transp. Rev. 142, 102056. http://dx.doi.org/10.1016/j.tre.2020.102056, URL: https://www.sciencedirect.com/science/article/pii/S1366554520307079.

He, Y., Liu, Z., Song, Z., 2022a. Integrated charging infrastructure planning and charging scheduling for battery electric bus systems. Transp. Res. Part D: Transp. Environ. 111, 103437. http://dx.doi.org/10.1016/j.trd.2022.103437, URL: https://www.sciencedirect.com/science/article/pii/S1361920922002632.

He, Y., Liu, Z., Song, Z., 2023. Joint optimization of electric bus charging infrastructure, vehicle scheduling, and charging management. Transp. Res. Part D: Transp. Environ. 117, 103653. http://dx.doi.org/10.1016/j.trd.2023.103653, URL: https://www.sciencedirect.com/science/article/pii/S1361920923000500.

He, J., Yan, N., Zhang, J., Yu, Y., Wang, T., 2022b. Battery electric buses charging schedule optimization considering time-of-use electricity price. J. Intell. Connect. Veh. 5 (2), 138–145. http://dx.doi.org/10.1108/JICV-03-2022-0006.

Hu, H., Du, B., Liu, W., Perez, P., 2022. A joint optimisation model for charger locating and electric bus charging scheduling considering opportunity fast charging and uncertainties. Transp. Res. Part C: Emerg. Technol. 141, 103732. http://dx.doi.org/10.1016/j.trc.2022.103732, URL: https://www.sciencedirect.com/science/article/pii/S0968090X2200167X.

Jahangir, M.H., Fakouriyan, S., Vaziri Rad, M.A., Dehghan, H., 2020. Feasibility study of on/off grid large-scale PV/WT/WEC hybrid energy system in coastal cities: A case-based research. Renew. Energy 162, 2075–2095. http://dx.doi.org/10.1016/j.renene.2020.09.131, URL: https://www.sciencedirect.com/science/article/pii/S0960148120315573.

Kermani, M., Adelmanesh, B., Shirdare, E., Sima, C.A., Carnì, D.L., Martirano, L., 2021. Intelligent energy management based on SCADA system in a real microgrid for smart building applications. Renew. Energy 171, 1115–1127. http://dx.doi.org/10.1016/j.renene.2021.03.008, URL: https://www.sciencedirect.com/science/article/pii/S0960148121003566.

Kermani, M., Chen, P., Göransson, L., Bongiorno, M., 2022. A comprehensive optimal energy control in interconnected microgrids through multiport converter under N-1 criterion and demand response program. Renew. Energy 199, 957–976. http://dx.doi.org/10.1016/j.renene.2022.09.006, URL: https://www.sciencedirect.com/science/article/pii/S0960148122013428.

Li, B., Chen, Y., Wei, W., Huang, S., Mei, S., 2021. Resilient restoration of distribution systems in coordination with electric bus scheduling. IEEE Trans. Smart Grid 12 (4), 3314–3325. http://dx.doi.org/10.1109/TSG.2021.3060801.

Li, W., He, Y., Hu, S., He, Z., Ratti, C., 2024. Planning dynamic wireless charging infrastructure for battery electric bus systems with the joint optimization of charging scheduling. Transp. Res. Part C: Emerg. Technol. 159, 104469. http://dx.doi.org/10.1016/j.trc.2023.104469, URL: https://www.sciencedirect.com/science/article/pii/S0968090X2300459X.

Lin, Y., Zhang, K., Shen, Z.-J.M., Ye, B., Miao, L., 2019. Multistage large-scale charging station planning for electric buses considering transportation network and power grid. Transp. Res. Part C: Emerg. Technol. 107, 423–443. http://dx.doi.org/10.1016/j.trc.2019.08.009, URL: https://www.sciencedirect.com/science/article/pii/S0968090X18312105.

Liu, K., Gao, H., Liang, Z., Zhao, M., Li, C., 2021. Optimal charging strategy for large-scale electric buses considering resource constraints. Transp. Res. Part D: Transp. Environ. 99, 103009. http://dx.doi.org/10.1016/j.trd.2021.103009, URL: https://www.sciencedirect.com/science/article/pii/S1361920921003072.

Liu, Z., Song, Z., He, Y., 2019. Economic analysis of on-route fast charging for battery electric buses: Case study in utah. Transp. Res. Rec. 2673 (5), 119–130. http://dx.doi.org/10.1177/0361198119839971.

Mirzaei, M.A., Yazdankhah, A.S., Mohammadi-Ivatloo, B., Marzband, M., Shafie-khah, M., Catalão, J.P., 2019. Stochastic network-constrained co-optimization of energy and reserve products in renewable energy integrated power and gas networks with energy storage system. J. Clean. Prod. 223, 747–758. http://dx.doi.org/10.1016/j.jclepro.2019.03.021, URL: https://www.sciencedirect.com/science/article/pii/S0959652619307048.

Moghaddam, Z., Ahmad, I., Habibi, D., Masoum, M.A.S., 2019. A coordinated dynamic pricing model for electric vehicle charging stations. IEEE Trans. Transp. Electr. 5 (1), 226–238. http://dx.doi.org/10.1109/TTE.2019.2897087.

Mohamed, M., Farag, H., El-Taweel, N., Ferguson, M., 2017. Simulation of electric buses on a full transit network: Operational feasibility and grid impact analysis. Electr. Power Syst. Res. 142, 163–175. http://dx.doi.org/10.1016/j.epsr.2016.09.032, URL: https://www.sciencedirect.com/science/article/pii/S0378779616303959.

Najafi, A., Masoudian, A., Mohammadi-Ivatloo, B., 2020. Optimal capacitor placement and sizing in distribution networks. In: Pesaran Hajiabbas, M., Mohammadi-Ivatloo, B. (Eds.), Optimization of Power System Problems : Methods, Algorithms and MATLAB Codes. Springer International Publishing, Cham, pp. 75–101. http://dx.doi.org/10.1007/978-3-030-34050-6_4.

Nath, R.B., Rambha, T., Schiffer, M., 2024. On the impact of co-optimizing station locations, trip assignment, and charging schedules for electric buses. Transp. Res. Part C: Emerg. Technol. 167, 104839. http://dx.doi.org/10.1016/j.trc.2024.104839, URL: https://www.sciencedirect.com/science/article/pii/S0968090X24003607.

Nordpool, 2023. Nordpool. Available at: https://www.nordpoolgroup.com/.

Ong, S., Campbell, C., Denholm, P., Margolis, R., Heath, G., 2013. Land-Use Requirements for Solar Power Plants in the United States. Technical Report NREL/TP-6A20-56290, National Renewable Energy Laboratory (NREL), Golden, CO, USA, URL: https://www.nrel.gov/docs/fy13osti/56290.pdf.

Perumal, S.S., Lusby, R.M., Larsen, J., 2022. Electric bus planning & scheduling: A review of related problems and methodologies. European J. Oper. Res. 301 (2), 395–413. http://dx.doi.org/10.1016/j.ejor.2021.10.058, URL: https://www.sciencedirect.com/science/article/pii/S0377221721009140.

Pragaspathy, S., Aravindh, G., Kannan, R., Dhivya, K., Karthikkumar, S., Karthikeyan, V., 2022. Advanced control strategies for the grid integration of wind energy system employed with battery units. In: 2022 International Conference on Power, Energy, Control and Transmission Systems. ICPECTS, pp. 1–5. http://dx.doi.org/10.1109/ICPECTS56089.2022.10046771.

Raza, M., Masud, A.R., Hussain, A., Lal, R.M., 2023. Bus selection index for distributed generators placement and sizing in the electrical network. Automatika 64 (2), 225–238. http://dx.doi.org/10.1080/00051144.2022.2130257.

Ren, H., Ma, Z., Ming Lun Fong, A., Sun, Y., 2022. Optimal deployment of distributed rooftop photovoltaic systems and batteries for achieving net-zero energy of electric bus transportation in high-density cities. Appl. Energy 319, 119274. http://dx.doi.org/10.1016/j.apenergy.2022.119274, URL: https://www.sciencedirect.com/science/article/pii/S0306261922006316.

Shaheen, A., Elsayed, A., El-Sehiemy, R.A., Abdelaziz, A.Y., 2021. Equilibrium optimization algorithm for network reconfiguration and distributed generation allocation in power systems. Appl. Soft Comput. 98, 106867. http://dx.doi.org/10.1016/j.asoc.2020.106867, URL: https://www.sciencedirect.com/science/article/pii/S156849462030805X.

Taşkin, Z.C., 2011. Benders decomposition. In: Wiley Encyclopedia of Operations Research and Management Science. John Wiley & Sons, Ltd, http://dx.doi.org/10.1002/9780470400531.eorms0104, URL: https://onlinelibrary.wiley.com/doi/abs/10.1002/9780470400531.eorms0104, arXiv:https://onlinelibrary.wiley.com/doi/pdf/10.1002/9780470400531.eorms0104.

Ufine Battery, 2024. How long do lithium batteries last? URL: https://www.ufinebattery.com/blog/how-long-do-lithium-batteries-last/#:~:text=Let's%20explore%20some%20common%20types,usage%20patterns%20and%20environmental%20conditions. (Accessed 02 December 2024).

U.S. Energy Information Administration (EIA), 2024. Solar energy and the environment. URL: https://www.eia.gov/energyexplained/solar/solar-energy-and-the-environment.php. (Accessed 02 December 2024).

Västtraffik, 2023. Västtraffik. Available at: https://www.vasttrafik.se.

Verbrugge, B., Hasan, M.M., Rasool, H., Geury, T., El Baghdadi, M., Hegazy, O., 2021. Smart integration of electric buses in cities: A technological review. Sustainability 13 (21), http://dx.doi.org/10.3390/su132112189, URL: https://www.mdpi.com/2071-1050/13/21/12189.

Wang, S., Chen, S., Ge, L., Wu, L., 2016. Distributed generation hosting capacity evaluation for distribution systems considering the robust optimal operation of OLTC and SVC. IEEE Trans. Sustain. Energy 7 (3), 1111–1123. http://dx.doi.org/10.1109/TSTE.2016.2529627.

Wang, X., Song, Z., Xu, H., Wang, H., 2023. En-route fast charging infrastructure planning and scheduling for battery electric bus systems. Transp. Res. Part D: Transp. Environ. 117, 103659. http://dx.doi.org/10.1016/j.trd.2023.103659, URL: https://www.sciencedirect.com/science/article/pii/S1361920923000561.

Wu, X., Feng, Q., Bai, C., Lai, C.S., Jia, Y., Lai, L.L., 2021. A novel fast-charging stations locational planning model for electric bus transit system. Energy 224, 120106. http://dx.doi.org/10.1016/j.energy.2021.120106, URL: https://www.sciencedirect.com/science/article/pii/S0360544221003558.

Wu, C., Wang, T., Zhou, D., Cao, S., Sui, Q., Lin, X., Li, Z., Wei, F., 2023. A distributed restoration framework for distribution systems incorporating electric buses. Appl. Energy 331, 120428. http://dx.doi.org/10.1016/j.apenergy.2022.120428, URL: https://www.sciencedirect.com/science/article/pii/S0306261922016853.

Zeng, Z., Qu, X., 2023. What's next for battery-electric bus charging systems. Commun. Transp. Res. 3, 100094. http://dx.doi.org/10.1016/j.commtr.2023.100094, URL: https://www.sciencedirect.com/science/article/pii/S2772424723000057.

Zhang, L., Zeng, Z., Gao, K., 2022. A bi-level optimization framework for charging station design problem considering heterogeneous charging modes. J. Intell. Connect. Veh. 5 (1), 8–16. http://dx.doi.org/10.1108/JICV-07-2021-0009.

Zhao, M., Shi, J., Lin, C., Zhang, J., 2018. Application-oriented optimal shift schedule extraction for a dual-motor electric bus with automated manual transmission. Energies 11 (2), http://dx.doi.org/10.3390/en11020325, URL: https://www.mdpi.com/1996-1073/11/2/325.

Zhou, Y., Meng, Q., Ong, G.P., Wang, H., 2024. Electric bus charging scheduling on a bus network. Transp. Res. Part C: Emerg. Technol. 161, 104553. http://dx.doi.org/10.1016/j.trc.2024.104553, URL: https://www.sciencedirect.com/science/article/pii/S0968090X24000743.

Zhou, Y., Wang, H., Wang, Y., Li, R., 2022. Robust optimization for integrated planning of electric-bus charger deployment and charging scheduling. Transp. Res. Part D: Transp. Environ. 110, 103410. http://dx.doi.org/10.1016/j.trd.2022.103410, URL: https://www.sciencedirect.com/science/article/pii/S136192092200236X.